

# RESEARCH MEMORANDUM

AIR-FLOW AND POWER CHARACTERISTICS OF THE  
LANGLEY 16-FOOT TRANSONIC TUNNEL  
WITH SLOTTED TEST SECTION

By Vernon G. Ward, Charles F. Whitcomb,  
and Merwin D. Pearson

Langley Aeronautical Laboratory  
Langley Field, Va.

NATIONAL ADVISORY COMMITTEE  
FOR AERONAUTICS  
WASHINGTON

July 21, 1952  
Declassified July 26, 1957

## NATIONAL ADVISORY COMMITTEE FOR AERONAUTICS

## RESEARCH MEMORANDUM

## AIR-FLOW AND POWER CHARACTERISTICS OF THE

## LANGLEY 16-FOOT TRANSONIC TUNNEL

## WITH SLOTTED TEST SECTION

By Vernon G. Ward, Charles F. Whitcomb,  
and Merwin D. Pearson

## SUMMARY

The Langley 16-foot high-speed tunnel, redesigned, repowered, and designated as the Langley 16-foot transonic tunnel was placed in operation in December 1950. The initial investigation of the flow characteristics in this facility included: establishment of acceptable uniform Mach number distributions in the model test region through the transonic Mach number range to 1.08, initial calibration of the resultant flow, effect of variations in wall divergence and diffuser entrance shape in regard to uniformity of flow and required horsepower, and general consideration of the mixing region and boundary-layer flows along the test section periphery. In addition, a comparison of power requirements for three similar transonic tunnels of widely varying scale is included.

The results from this investigation indicate for a particular tunnel configuration the attainment of acceptably uniform transonic flows which are continuously variable up to the highest supersonic Mach number attainable with the design power. The power requirement per unit of throat cross-sectional area to obtain a given Mach number in this large-scale facility is somewhat less than previously reported for similar transonic tunnels of smaller scale.

## INTRODUCTION

An investigation of solid blockage interference in a wind tunnel with walls slotted in the direction of flow was first reported in reference 1. Such a slotted tunnel minimized the interference due to solid blockage of relatively large test models and eliminated tunnel choking.

It was demonstrated in reference 1 that a slotted test section could provide Mach numbers which are continuously variable through 1.0 to low supersonic values merely by varying the input power. The supersonic Mach number distributions in the model test region, however, were nonuniform and unacceptable for model testing. The rectangular slot plan form employed in the slotted test section of reference 1 was later revised to a gradually tapered slot plan form as reported in reference 2. This tapered slot plan form greatly improved the uniformity of the supersonic flows in the test region throughout the supersonic Mach number range from 1.0 to 1.26. Additional modification of this type of slot plan form in the Langley 8-foot transonic tunnel, reported in reference 3, further improved the uniformity of the supersonic flows such that the Mach number variations in the flow were no greater than those experienced in the most carefully designed and constructed two-dimensional supersonic solid nozzles.

The Langley 16-foot high-speed tunnel was extensively modified and repowered for slotted-tunnel operation in order to utilize the favorable aerodynamic characteristics of the slotted test section and to provide a facility in which experimental data could be obtained from large-scale models operating through sonic velocity.

Investigation of several slotted-test-section parameters, generally similar to those reported in reference 3, resulted in a particular configuration for this facility which produces flows of excellent quality that are continuously variable and controllable throughout the test Mach number range to a supersonic value of 1.08. General flow characteristics, together with power considerations, are also presented. This large-scale facility, designated the Langley 16-foot transonic tunnel, was first placed in operation December 6, 1950.

## DESIGN MODIFICATIONS AND SURVEY INSTRUMENTATION

### Tunnel Redesign

Figure 1 presents a general schematic view of the Langley 16-foot transonic tunnel and its pertinent survey instrumentation. The location of any part of the tunnel is measured parallel to the two long legs of the tunnel and relative to station zero which is noted in figure 1. The station numbers represent distances in feet. The major parts of the original Langley 16-foot high-speed tunnel which were redesigned are: the section between stations 43 and 179 which includes the entrance and test sections and a part of the diffuser, the section from stations 285 through the first set of turning vanes, the power section and the second set of turning vanes to station 283 in the return passage, and the air-exchange tower. Other minor modifications made to the tunnel were for structural purposes.

Entrance section.- The entrance section extends from station 43 to station 107. Because of the circular shape of the quiescent chamber and the octagonal shape of the test section, a transition region is necessary and extends from station 43 to station 70 (see fig. 1). The remainder of the entrance section has an octagonal cross section. The part of the entrance section between stations 95.5 and 107, designated the entrance liner, is fabricated of flexible machined plates. These plates are mounted on jackscrews to facilitate adjustment of the entrance liner contour to meet construction tolerances.

Test section.- The test section is located between stations 107 and 154, and is shown in the detailed sketch of figure 2. Figure 3 is a photograph of the test section with the access hatch in the raised position. The main components of the test section, as noted in the figures, are the flats or walls, the open slots, and the diffuser entrances, all of which are completely enclosed in a sealed cylindrical tank the diameter of which is twice the effective diameter or 32 feet. The flats make up the sides of the octagonal-shaped test section and eight slots comprising approximately  $1/8$  of the total periphery are located at the corners between the flat sides. The diffuser entrances provide a terminal point for the slots.

The flats consist of a continuous sheet of steel from station 107 at the geometric minimum (the area of which is equal to 199.15 sq ft) to station 154 in the closed diffuser. Each steel plate is backed by two reinforcing truss systems extending from station 112 to 138 and from station 140 to 154, such as to maintain these parts of the walls straight and flat. The wall divergence in the test section can be varied remotely by changing the slope of the forward straight portion of the flats relative to the tunnel center line. An outward radial motion is applied to the flats at station 138 and the necessary bending of the flats due to this motion occurs over the unsupported sections of the flats centered about station 110 and 139. When the wall divergence is varied, the resultant sliding action occurs at the downstream end of the flats (station 154). A part of the wall-divergence drive mechanism may be seen in the background between a flat and the tank wall in figure 3. The rearward straight portions of the flats downstream of station 140 have a slope of approximately  $2.75^\circ$  with respect to the center line of the tunnel when the divergence of the flats between stations 112 and 138 is zero.

The open slots are located at the corners between adjacent flats. The radial boundaries of the slot are established by slot-edge skirts which are normal to the flat surfaces and extend two feet into the tank. These skirts provide a radial slot relief of  $45^\circ$ . The edge skirts maintain a near sharp juncture with the flat surface and extend at approximately constant slot width along the entire slot length (see fig. 3).

The shape of the upstream part of the slot may be conveniently altered by means of inserts.

The diffuser entrances are located at the downstream end of the slots below the surfaces of the flats. Two geometrically different configurations were used in this investigation, and sketches illustrating their shapes and dimensions in a plane passing through the tunnel center line and the slot center line are shown in figure 4. All surfaces of both diffuser entrances are normal to this plane and are terminated by intersection with the slot-edge skirts of adjacent flats. The original diffuser entrance, similar to that reported in references 1 and 2, extends from station 142, where it intersects the tank wall, to station 154, at which point it becomes tangent to a plane intersecting the edges of adjacent flats. At station 154, where the periphery of the tunnel becomes completely closed, the area is approximately 20 percent greater than that of the station of minimum area, 107. The revised diffuser entrance, the design of which was based upon a similar configuration presented in reference 3, and the results of studies subsequently described in this paper, extends from station 139 downstream to station 146 (fig. 4). The surface of the revised entrance configuration toward the tunnel center line is parallel to the tunnel axis from the leading edge at station 139 to station 141.5. The surface is then shaped as illustrated in figure 4 and becomes tangent to a plane intersecting the edges of adjacent flats at station 146. The area of the irregular tunnel cross section at the leading edge of the revised diffuser entrance is approximately 5 percent greater than the minimum area at station 107; whereas the area at station 146 where the tunnel periphery is now completely closed is approximately 9 percent more than the minimum area.

In order to provide for the installation and removal of models and test instrumentation in the test section, the upper part of the tank together with the top flat and the two adjacent flats are removable as a complete unit. With this hatch in the raised position (fig. 3), an access region is provided which equals the width of the test section, 15.5 feet diametrically across flats, and extends about 52 feet in length from approximately station 106 to station 158.

Test models may be mounted in the test section by means of either a sting support strut or a reflection-plane support system. The profile view of the sting support strut is shown in figures 1 and 2. A model mounted on this support strut is shown in the photograph of figure 3. The base of the strut is mounted on a curved track located beneath the bottom flat. Traverse along this track allows remote variation of the pitch attitude of a test model about station 134 at the center line of the tunnel. The reflection-plane support system (not shown in this paper) may be mounted in the opening in flat number 6 provided by the removal of the schlieren window (figs. 2 and 3).

Two schlieren windows 3 feet wide and 6 feet long are located opposite each other in the vertical flats (flats number 2 and 6, fig. 2) of the test section between station 131 and station 137. Two similar windows are located in the tank walls directly aligned with those in the test section flats and permit, together with the windows in the flats, visual or schlieren observations of the test region.

General lighting of the test region is provided by units of sealed beam lights located on the tank wall (fig. 3). These lights are directed through the slots so as to illuminate the test model.

Diffuser sections.- A large part of the original diffuser and return passage is utilized in the present tunnel configuration without modification. However, the section between stations 154 and 179 was redesigned to provide a transition from the octagonal shape of the test section to the circular shape of the diffuser. In addition, two diffuser sections of circular cross section were required between diffuser stations 285 and 326 and between the corresponding return-passage stations 283 and 326 to adapt the unmodified parts of the diffuser to the redesigned power section.

Power section.- The redesigned power section extends from station 326 in the diffuser to the corresponding station 326 in the return passage with its center line located at station 349 (fig. 1) and at right angles to the diffuser and return-passage center lines. The first and second sets of turning vanes are located at each corner of the 34-foot constant-diameter passage. The nacelle of 20-foot outside diameter at the drive fans (see dotted lines in fig. 1) allows a 7-foot annular section for the two drive fans. The 25-blade upstream fan and 26-blade downstream fan are counterrotating and each is powered by a 30,000-horsepower motor externally mounted from the ends of the power section. The airfoil fairing over one drive shaft, as well as the nacelle, support struts, and drive fans are noted in the photograph presented as figure 5. The tunnel shell in this region is completely enclosed in a massive concrete structure in order to reduce the vibration and noise level of the power section. In addition, each end of the power-section structure is isolated from the remaining tunnel sections by means of rubber gaskets (station 326, fig. 1).

Air-exchange section.- Modifications to the air-exchange section included the installation of oil-bath type of air filters in the intake system, the unification of each set of intake and exit vane louvers, and the installation of noise-reduction baffles in both the intake and exit systems. The intake and exit vane louvers were redesigned such that each set of vanes may be manually adjusted as a unit instead of the individual manual vane adjustment previously required for the 36 vanes of each set. This manual adjustment presently limits changes in vane

openings to delays between tests. Subsequent modification will provide remote control for variation of vane opening at any time during a run.

### Survey Instrumentation

Wall orifices.- Instrumentation used to determine the flow characteristics in the redesigned 16-foot tunnel included static pressure orifices in the walls or flats of the entrance liner and test section. The locations of these static orifices are shown in figure 2. The diameter of the wall orifices is 0.020 inch. On flat number 1 in the entrance liner from station 95.5 to 106.75, 23 static orifices are spaced about 6 inches apart and are located 6 inches off the center line of the flat. This line of orifices is continued along flat number 1 in the test section with 93 static orifices similarly spaced between stations 107.5 and 153.5. On the revised diffuser entrance, between flats 1 and 2, 39 static orifices, most of which are spaced 6 inches apart, are located between station 139.1 and station 145.2. Twenty-one of these orifices are located on the diffuser entrance surface nearest the tunnel center line and the remainder are on the tank-side surface. The calibration orifices are located in the tank wall behind flats 2, 6, and 8 at station 110.5.

Survey tube on center line.- Static pressure measurements along the center line of the test section were obtained by means of orifices 0.020 inch in diameter located in a long axial survey tube 4 inches in diameter. Figure 6 presents photographs of the upstream and downstream views of the survey tube mounted in the test section. The survey tube extended from station 74.5 in the entrance cone downstream to station 141.5 in the test section where it was secured at the model support strut (figs. 2 and 6(b)). The upstream end of the tube is supported by eight wire cables in tension (fig. 6(a)). The deflection of the tube due to its own weight produced a maximum slope of the tube axis which did not exceed  $\pm 1^\circ$ . The 54 static pressure orifices, spaced 9 inches apart, are located between station 100.25 and station 140.

Total-pressure rake.- Stagnation-pressure measurements were obtained from four shielded total-pressure tubes located at the upstream end of the quiescent chamber approximately on the center line of the tunnel.

Boundary-layer rakes.- A rake of 34 total-pressure tubes was mounted radially in the slot between flats 1 and 8 such that approximately 4 feet of its length extended from the intersection line of the planes containing adjacent flats toward the center of the stream and approximately 3 feet into the tank (fig. 2). The rake was movable to various longitudinal positions along the slotted part of the test section. In addition, two total-pressure rakes, 6 inches and 12 inches in length, were mountable on a flat or through a slot at stations near the slot origin.



Angle-of-attack vane.- A free-floating vane of approximately 3-inch span (fig. 6 (c)) was used to measure the free-stream flow angularity relative to the tunnel longitudinal axis at the center of the test region.

## AIR-FLOW AND POWER CHARACTERISTICS

### Development of Uniform Flows

The results of slotted tunnel flow uniformity investigations presented in references 2 and 3 indicated that the slot-entrance plan-form design was particularly important to the development of uniform supersonic flows. Reference 3 also indicated that large wall-divergence angles apparently exerted a predominate influence on the development of low supersonic flows and resulted in flows unsuitable for model testing. These parameters of slot-plan-form shape and wall-divergence angle, which were conveniently variable in the redesigned 16-foot slotted test section, are studied in some detail in the present investigation.

Effect of slot shape.- Six slot-plan-form shapes, specified in figure 7, were investigated during the initial operation of the 16-foot transonic tunnel. The slot plan forms numbered 1, 9, and 11 correspond, with slight modification, to the most promising slot shapes tested in the 8-foot transonic tunnel and are of the same number (ref. 3). Three additional shapes, arbitrarily numbered 16, 17, and 18, were designed on the basis of test results of the original shapes.

Wall and center-line Mach number distributions in the test section are presented throughout the test Mach number range in figures 8 to 12 for several of the slot-plan-form shapes. All other test-section components remain fixed for these tests, except for variation in test-section-wall-divergence angle  $\delta$  which is noted on the figures. A schematic drawing of the test-section configuration is also included at the top of each figure. The stream Mach number  $M$  is presented as the average of the maximum and minimum local Mach numbers  $M_l$  on the center line of the stream over a length of one-tunnel effective diameter, from station 122 to station 138; and the Mach number variation  $\Delta M$  is one-half the difference between the maximum and minimum Mach numbers over this same length.

In figure 8 is presented the test-section Mach number distributions obtained with slot-entrance plan form number 1 (fig. 7). This slot entrance is the basic long-tapered slot shape used in flow uniformity investigations reported in references 2 and 3 for slotted test sections. The Mach number distributions developed by this slot entrance with



0° 5' wall divergence are uniform within  $\pm 0.005$  in the subsonic and transonic range to a tunnel Mach number of approximately 1.034. At a Mach number of 1.077, the variation in the Mach number distribution is  $\pm 0.010$ . This Mach number was obtained with a maximum available horsepower. At this same power, a Mach number of 1.096 was obtained by increasing the wall divergence to 0° 10' and the Mach number variation increased to  $\pm 0.018$ .

In figure 9 is shown the tunnel Mach number distributions obtained with slot-entrance plan form number 11 (fig. 7). This slot-entrance has an initial rate of opening equal to that of slot-entrance number 1. The rate of slot opening then decreases until it is approximately one-half that of slot plan form number 1. The decrease in the rate of slot opening was designed to reduce the Mach number variations in the test region. The Mach number distributions developed by this slot shape with 0° 5' wall divergence are acceptable in both the subsonic and supersonic ranges to a tunnel Mach number of 1.072. At a Mach number of 1.072, the highest obtainable with 0° 5' wall divergence, the Mach number variation  $\pm 0.005$  is approximately one-half that of slot entrance number 1. When the wall-divergence angle was increased to 0° 10' at the same power condition, the stream Mach number increased from 1.072 to 1.090 causing an increase in the Mach number variation of 0.011 or a total Mach number variation  $\pm 0.016$ . A Mach number of 1.119 was obtained with a wall divergence of 0° 10' when the power was increased above that which is normally available to the tunnel.

Although the supersonic flows in the test region with slot number 11 and a 5-minute wall divergence were of desired uniformity, emphasis was directed toward improving the uniformity of the flows at higher Mach numbers obtainable with 0° 10' wall divergence. It was believed that a decrease in initial rate of slot opening might counteract flow accelerations associated with the increased wall divergence. In order to determine the degree of reduction of slot opening necessary, slot shape number 9, which produced a very uniform flow and was utilized as the basic slot shape for the design of the final 8-foot tunnel slot entrance, was tested at 10-minute wall divergence.

Slot-entrance plan form number 9 (fig. 7) has a linear rate of opening one-half that of slot entrance number 1. Figure 10 presents the Mach number distributions for slot number 9 with 0° 10' wall divergence. The subsonic distributions developed by this entrance are uniform within acceptable values of Mach number variation. The supersonic distributions, however, indicate an increasing Mach number variation as the Mach number is increased from 1.036 to 1.103. In comparison with the distributions of slot plan form number 11 at 0° 10' wall divergence (fig. 9), the Mach number variations of slot entrance number 9 are of the same order of magnitude. Although the initial rate of development of the flow for slot number 9 was somewhat reduced as anticipated, the

same order Mach number variations did not positively indicate whether the rate of slot opening was sufficiently reduced to compensate for the increase in tunnel area associated with the  $0^\circ 10'$  wall-divergence condition. In order to obtain a positive indication of the effect of rate of flow development on the flow uniformity at the  $0^\circ 10'$  wall-divergence condition, the rate of slot opening was appreciably reduced in slot shape number 16.

The linear rate of opening of slot entrance number 16 was reduced to one-fourth that of slot entrance number 9, or one-eighth that of slot number 1 (fig. 7). Figure 11 presents the Mach number distributions for slot entrance number 16 with  $0^\circ 10'$  wall divergence. The subsonic distributions are uniform and within acceptable tolerances of Mach number variation. All of the supersonic distributions indicate some nonuniformity greater than desired and show no improvement over the supersonic distribution developed by slot-entrance plan form number 9 even though the rate of initial development of the flow is appreciably reduced.

Slot entrance number 17 was modified only slightly in comparison with slot plan form number 16 in order to reduce the abruptness of the plan-form fairing between stations 117.5 and 122. The effects of this minor change upon the uniformity of the distributions were negligible, and the distributions are omitted.

Several general observations were noted from the preceding data: (1) the decrease in the initial rate of slot opening relative to that of plan form number 1 did not improve the uniformity of the resultant supersonic flows either at  $0^\circ 5'$  or  $0^\circ 10'$  wall divergence; (2) the most uniform supersonic flows at the  $0^\circ 5'$  wall-divergence position were established with slot shape number 11, which opened initially at the rate of slot number 1 but was soon decreased to one-half this rate; (3) increases in maximum Mach number at a given power were obtained by increasing the wall divergence although the resultant flows were not uniform; (4) slot shape number 16, although exhibiting an unacceptable distribution, showed, by a decrease in the rate of establishment of the supersonic flow, that some initial control of the flow was possible with  $0^\circ 10'$  wall divergence. Considerations of these observations indicated that some improvement in the uniformity of supersonic flows might be obtained at increased wall divergence by allowing an initially rapid acceleration followed by a decreased acceleration to the final Mach number.

Slot-plan-form shape number 18 was designed, therefore, so that its contour was similar to slot shape number 11 over the upstream part of the slot entrance and similar to slot shape number 16 over the downstream part. In addition, the location of the origin of plan form number 18 was moved upstream from station 110 to station 107.5. This upstream displacement of the slot origin into a region of nearly constant Mach number and of geometrically constant area was made in an effort to

increase the slot entrance length without altering appreciably other tunnel characteristics.

The initial rate of opening of slot-entrance plan form number 18 is slightly greater than that of slot entrance numbers 1 and 11 (fig. 7). At station 108.5 the rate of opening becomes less than that of numbers 1 and 11 and continues to decrease until at station 115 the rate of opening becomes equal to the initial rate of plan form number 16, or one-eighth that of plan form number 1. This rate is maintained up to station 119.5 and finally becomes the same as that of slot entrance number 9 at station 122.75. The Mach number distributions for slot number 18 with a wall divergence of  $0^\circ 10'$  were nonuniform at the supersonic values, having Mach number variations of the same order as slots number 9, 16, and 17. Inasmuch as the uniformity of the distributions for the 10-minute divergence was not acceptable, the data are not presented. The distributions at  $0^\circ 5'$  wall divergence were, however, uniform throughout the Mach number range and are presented in figure 12. The maximum available horsepower gave a tunnel Mach number of 1.075 with 5-minute wall divergence. The Mach number variations over the entire Mach number range to 1.075 are within  $\pm 0.006$ . Although slot-entrance plan form number 18 was somewhat different from slot shape number 11, it developed as uniform a flow over the same Mach number range for the same wall divergence. In view of the uniformity of these resultant flows, slot shape number 18 with a wall divergence of 5 minutes was selected as the final operating configuration for this facility.

Additional characteristics of the flow are noted in figures 8 to 12. In the part of the entrance liner which was surveyed, the local Mach number in the center of the stream is somewhat lower than that indicated at the wall for a particular station. This difference in local Mach number, which is evident in all preceding distributions, tends to decrease as the flow approaches the minimum area at station 107 and indicates a near-constant velocity across the station of minimum area for supersonic as well as subsonic Mach numbers. At supersonic values, the slope of the Mach number distributions in this region approaches zero upstream of station 107 and then increases again as the flow enters the slotted part of the test section. The range of tunnel stations over which this near-zero slope occurs increases slightly as the initial width of the slot-entrance plan form decreases. This near-zero slope condition is less evident when the slot origin is located at station 107.5 (see slot number 18 in fig. 12).

The effective nozzle part of the test section has been arbitrarily designated as the region in which the supersonic flows are developed. The slope of the Mach number distribution in this region (previously designated as the rate of flow development) is a function of the slot-entrance plan form. As the rate of opening of the slot entrance decreased

for a constant wall divergence and tunnel Mach number, the slope of the Mach number distribution curve decreased.

The slotted diffuser is the part of the test section from the downstream end of the test region, station 138, to the station where the diffuser entrance is tangent to the surface of the closed diffuser, station 146. A local apparent Mach number peak along the tunnel wall occurs in the upstream part of this region both subsonically and supersonically, as well as along the center line supersonically. Subsonically, the center line Mach numbers decrease in this region.

The downstream part of the test section includes a part of the closed diffuser. It may be noted in figure 8 (at  $M = 1.096$ ,  $\delta = 0^\circ 10'$  and  $M = 1.077$ ,  $\delta = 0^\circ 5'$ ) that a near duplication of local Mach number distribution occurs in this closed region of the diffuser when a variation in wall divergence is made at a constant horsepower condition.

Effect of wall divergence. - The ability to vary remotely the wall-divergence angle permitted an extensive investigation of the effects of such variations on the Mach number distributions in the tunnel.

The effects of wall divergence upon the Mach number gradient in the test region for Mach numbers of approximately 0.95 and 1.05 and for wall divergences of  $0^\circ 0'$ ,  $0^\circ 5'$ , and  $0^\circ 10'$  are presented in figure 13. These effects are illustrated by means of wall and center-line longitudinal Mach number distribution comparisons similar to those presented in figures 8 to 12. The tunnel configuration utilized slot plan form number 18 and the revised diffuser entrance. It may be noted that a slightly positive Mach number gradient exists in the test region for both the subsonic and supersonic Mach numbers at  $0^\circ$  wall divergence; whereas a slightly negative Mach number gradient exists for the  $0^\circ 10'$  wall-divergent position. Although these gradients in the test region are of the order of only 0.01, the  $0^\circ 5'$  wall-divergence angle appears to compromise between the  $0^\circ$  and the  $0^\circ 10'$  positions, a condition which indicates little or no gradient either subsonically or supersonically. It is also noted that the distribution for the  $0^\circ 10'$  wall divergence at Mach number 1.05 indicates a slight compression region following the initial expansion to the test Mach number. Also illustrated in this figure is the gradual reduction of the localized apparent Mach number increase over the two-foot faired region centered about station 139 as the wall divergence increases from  $0^\circ 0'$  to  $0^\circ 10'$ .

The effect of varying wall divergence upon the uniformity of flow in the test region was investigated at the top power condition of 62,000 horsepower. The Mach number distributions along the center line of the test section for several wall-divergence positions from  $0^\circ 0'$  to  $0^\circ 20'$  by 4-minute increments are presented in figure 14 with a Mach

number scale 2.5 times that shown in the preceding figures. If local irregularities thus magnified are discounted, it may be noted that, as the wall divergence increases from  $0^\circ 0'$  to  $0^\circ 20'$ , the local Mach number increases and flow variations become progressively large until a value of 0.05 is shown for the  $0^\circ 20'$  position. This variation or non-uniformity exists in the form of a gradual compression and reexpansion and occurs over a length of approximately three-fourths effective tunnel diameter. Ahead of this region, the flow appears to have expanded normally in the effective nozzle to produce a somewhat uniform flow over a region of approximately three-eighths effective tunnel diameter. The Mach number corresponding to the static pressure in the tank  $M_{\text{tank}}$ , which is presented for comparison, agrees well with the local Mach number in this region. The distribution for  $0^\circ 0'$  wall divergence indicates a slightly positive Mach number gradient with the apparent absence of a compression region for the 1.05 Mach number shown, and it is not known whether similar aforementioned nonuniformities would occur were higher Mach numbers attainable at this  $0^\circ 0'$  divergent position.

This investigation of the effects of variation of wall divergence has shown an increasing Mach number associated with an increase in wall divergence at constant power. The uniformity of flow, however, decreases with this increasing Mach number and, within the particular limits of slot shape and input power investigated, the most uniform and gradient-free flow is produced at a wall divergence of approximately 5 minutes.

### Test-Section Calibration

A calibration of the flow in the test section to determine the representative stream Mach number and degree of flow angularity is now presented.

Mach number calibration in test region.- A calibration of the Mach number in the test region, similar to the procedure of references 1, 2, and 4, utilized static-pressure measurements obtained with orifices at the tank surface located at station 110.5 behind flats number 2, 6, and 8 (fig. 2). These static-pressure values correspond nearly to the Mach number in the stream at all test conditions and are continuous through the sonic value. The results in reference 4 indicate that the presence of a model does not affect the model-removed calibration. The average stream Mach number along the center line of the test section between stations 131 and 137 is calibrated against the Mach number corresponding to the ratio of the aforementioned static pressure in the tank to the total pressure in the stream and is presented in figure 15. This method allows a nearly straight-line fairing which approaches a  $45^\circ$  slope. The representation of the stream Mach number by the average of pressures along the center line of the stream between stations 131 and 137 is

believed to be as accurate for this particular facility as the more detailed procedure followed in reference 4. Small variations in Mach number off the test-section center line can be inferred from the surveys of reference 4 and from the close agreement between the Mach number distributions of the wall and center line. The arbitrary 6-foot length between stations 131 and 137 allows a single calibration, as shown in figure 15, which has a maximum point deviation of  $\pm 0.002$  from the faired line over the entire test Mach number range.

Flow angularity in test region.- An indication of the test region free-stream flow angularity, relative to the tunnel longitudinal axis, was obtained from tests of a small free-floating angle-of-attack vane placed on the test section center line at tunnel station 134. Figure 16 presents the results of the vane tests in the pitch or vertical plane, over a Mach number range from 0.60 to 1.07 for two air-exchange louver or vane settings. (See fig. 1.) For a large or 34-inch air-exchange intake and exit-vane opening, an indicated upflow angle of  $0.40^\circ$  at a Mach number of 0.60 which decreases linearly to a value of  $0.25^\circ$  at a Mach number of 1.07 is shown. The results of a second air-exchange vane setting indicate a decrease to little or no test-region flow angularity over the same Mach number range. For this test, the exit-vanes which control the amount of tunnel air exchanged were open to 12 inches and all but six of the intake vanes were closed. These six, equally spaced about the tunnel periphery, were opened to a  $45^\circ$  angle which, because of their length beyond their hinge points, extended them far into the stream. This setting resulted in their use as large angle flaps to induce the cooling air supply into the center of the free stream. This vane-setting configuration is in use for current operation of the tunnel. A discussion of the tunnel air-exchange problems in connection with tunnel boundary-layer conditions is treated subsequently in the text.

The data for some of the first investigations in this tunnel had been prepared for publication prior to the stream-angle measurements and therefore do not include corrections for stream alinement.

### Supplementary Flow Investigations

Supplementary investigations of flow conditions at the surface of the diffuser entrance and in the mixing region and boundary layer were conducted in some detail and some general observations of these flow conditions are presented.

Flow conditions at diffuser entrance.- Two diffuser entrances were used in this phase of the investigation. The original diffuser entrance, installed during the period of extensive tunnel modification and repowering, was similar to the entrances used in references 1 and 2. With this entrance configuration installed, the Mach number distributions

along flat number 1 in the test section for Mach numbers of 0.7 and 0.92 are illustrated by the circular symbols in figure 17. The distributions in the test region appeared uniform, but little evidence of static-pressure recovery was shown from the rear of the test region to station 146. As the power consumption for this configuration appeared high enough to preclude attaining Mach numbers in excess of 1.0, possible design modifications of the test section to improve the power characteristics of the tunnel were considered. Preliminary investigations of various diffuser entrance configurations in the Langley 8-foot transonic tunnel (ref. 3) resulted in the development of a scoop-type diffuser entrance which provided a substantial reduction of required tunnel power. This available information in addition to visual flow studies made along the various tunnel surfaces in the vicinity of the original 16-foot transonic tunnel diffuser entrance (subsequently described in the present paper) was used in the design and installation of the revised diffuser entrance. (See fig. 4 and sketch at top of fig. 17.) The resultant Mach number distributions for the revised diffuser entrance at similar Mach numbers and at a supersonic value of 1.02 are shown for comparison in the same figure. A small positive Mach number gradient between stations 134 to 138 is favorably reduced with the revised diffuser entrance configuration. In addition, the local apparent Mach number peak which occurs over the faired transition from slotted test region to slotted diffuser, stations 138 to 140, is favorably reduced. Also indicated, with the installation of the revised diffuser entrance, is an increase in the static-pressure recovery over the region between stations 138 and 154. This increase in static-pressure recovery at station 154 is approximately 0.9 percent for an indicated test section Mach number 0.70 and approximately 3.6 percent for an indicated test section Mach number of 0.92. This increase in static-pressure recovery results in a stream Mach number increase from about 0.93 to 1.02 when the static pressure at station 154 is about equal for both entrance configurations.

A comparison of local pressure ratios  $p_l/H$  over the revised diffuser entrance with pressure ratios at similar longitudinal locations 6 inches from the center line of the flat are presented for several stream Mach numbers in figure 18. The pressure ratio in the tank  $p/H_{\text{tank}}$  is also included for comparison. The faired line with symbols represents the static pressures on the revised diffuser entrance, and the corresponding faired line without symbols represents the static pressures near the center line of one adjacent flat. The tailed symbols indicate lower surface of the diffuser entrance. It is noted that pressures over the upper surface of the entrance from approximately station 139.5 to station 140.5 are missing from these data. The fairing is, therefore, based upon previous similar measurements which were limited to stream Mach numbers less than 1.03. The figure indicates that the tank pressure, which corresponds nearly to the stream Mach number, has approximately the same value as that at the under surface of the entrance.



The pressures on the upper surface of the entrance appear to increase rapidly from this tank-pressure value until reaching a peak near station 143 and then to decrease rapidly to about station 145. This local-pressure reversal appears primarily over the reverse curve part of the diffuser entrance (see sketch at top of fig. 18). The pressures near the center line of the flat, although continuously increasing through the slotted part of the diffuser, appear to be influenced by the local-pressure reversal. Downstream of station 147, where the entrances have become tangent and the diffuser a closed section, the pressures at the two locations are approximately equal. This trend appears true for all Mach numbers both subsonic and supersonic. The general pressure patterns, both over the diffuser entrance and along the center line of the flat, appeared to progress continuously through the sonic range to a top Mach number of 1.08.

Figure 19 presents a similar comparison of pressures over the revised diffuser entrance for wall-divergence angles of  $0^\circ$ ,  $0^\circ 5'$ , and  $0^\circ 10'$  at stream Mach numbers near 0.95 and 1.05. The diffuser entrance remains fixed and the flats diverge as illustrated in the sketch included in the figure. The general pressure pattern, previously described in the discussion of figure 18, is evident for the three wall-divergence angles. It is recalled from previous figures that the indicated stream Mach number increases with increasing wall divergence for constant power. Figure 19 illustrates this same effect by indicating an increasing static pressure at station 153 as the wall divergence increases from  $0^\circ$  to  $0^\circ 10'$  for a given Mach number. The only apparent increase in the rate of pressure rise, and consequent gain in static-pressure recovery, for increasing wall divergence from  $0^\circ$  to  $0^\circ 10'$  occurs in the region of the straight part of the diffuser entrance between stations 139 and 141.5. These data included in figures 18 and 19 are believed to indicate that the revised diffuser entrance configuration is not necessarily the ultimate configuration either in the local pressure distribution or in its effect on power reduction by increasing static-pressure recovery. The fact that this diffuser entrance configuration increased the static pressure recovery appreciably and allowed stream Mach numbers up to 1.08 to be obtained with existing power facilities prompted immediate model tests with this revised configuration and delayed further modification until a future date.

Flow conditions in mixing region and boundary layer.- The general flow conditions in the mixing region of the slot and in the boundary layer of the flat are shown by means of total-pressure surveys made radially through the slot and from the surface of the flat for particular longitudinal positions and air-exchange vane louver openings. Local total pressures  $H_1$  were measured along a radius through the center line of the slot between flats number 1 and 8 at station 126.9 and are presented in figure 20 as a function of the stagnation total pressure in the quiescent chamber for several Mach numbers. The tunnel air-exchange

intake and exit-vane openings (fig. 1) were 12 inches. The slot shape is number 18. A 120-inch drop-body test model, with the sting mounted at  $\alpha = 0^\circ$  and its nose position at station 126, was mounted in the tunnel. The static-pressure ratio in the tank is included for comparison. The total pressure distributions radially through the slot are generally symmetrical about the intersection line of the planes containing the adjacent flats (hereafter designated as the intersection of the flats) for all Mach numbers. For the 1.07 Mach number distribution, no correction for total pressure loss through the bow waves ahead of the tubes on the rake is made ( $H_t/H$  correction is 0.0004 for normal shock). No losses in the stagnation total pressure in the free stream are evident until a point about 12 inches from the intersection of the flats, except for the two highest Mach numbers of 0.983 and 1.070 where a loss of about 0.001  $H_t/H$  appears between radial stations 32 and 12 inches. The total pressure ratio about 12 to 14 inches below the intersection of the flats corresponds to the static-pressure ratio in the tank for all Mach numbers except the highest of 1.07. At Mach number 1.07, the total-pressure ratio at this radial position is within 1 percent of the static-pressure ratio in the tank, but does not assume the corresponding tank pressure until radial station 22.

A similar plot with all conditions remaining fixed, except for an increase of the air-exchange intake and exit vane opening to 36 inches, the widest design opening possible, is shown in figure 21. The total pressure distributions are similar to those in figure 20 except for losses in total pressure from radial station 12 toward the center line of the stream. These total-pressure losses are negligible to a Mach number of approximately 0.60. Above this Mach number the losses progressively increase until the top Mach number of 1.054 where they approach 1.5-percent  $H_t/H$  at radial station 12 and gradually decrease to approximately 0.5-percent  $H_t/H$  at radial station 48. Stagnation temperature measurements made under the same test conditions, although doubtful because of possible reevaporation of condensed moisture from the thermocouples, indicate that a relatively cold layer of air, as induced by the air-exchange intake vanes, proceeds through the test region without complete mixing. The thickness of this cold layer is associated with the amount of vane opening. Consideration of these measurements for the 36-inch intake vane-opening configuration indicates that air-state conditions representing 100 percent or more relative humidity exist several feet toward the center line of the stream from the intersection of the flats. Such considerations, together with visible condensation in the vicinity of the slots, correlate with the aforementioned total pressure losses indicated in the figure.

A further comparison of the top Mach number distributions of figures 20 and 21 is shown in figure 22 for vane openings of 12 and 36 inches. The total pressure loss toward the center line of the stream

for the 36-inch vane opening condition, believed to be associated with the aforementioned problem of condensation, is more clearly illustrated when compared with the essentially less-free distribution of the 12-inch vane opening condition. Correction for total-pressure loss through bow waves ahead of the total-pressure tubes was not made for either distribution.

Total-pressure measurements presented thus far have been shown for tunnel longitudinal station 126.9 only. Figure 23 presents for a Mach number of approximately 1.07 similar data for stations 107.5, 126.9, and 136.9 for an air-exchange intake and exit-vane opening of 30 inches and with the 20-inch drop-body test model removed. Included also are radial measurements from the center line of one of the flats for the 107.5 station only. Station 107.5 is the origin of slot shape number 18, the configuration used for these measurements. Parts of these data were obtained neither simultaneously nor in the same radial plane, thereby limiting direct comparison. It may be noted from the figure, however, that the depth of the mixing region increases with increasing longitudinal station in the downstream direction, extending to approximately 16 inches inside the intersection of the flats and 22 inches outside of this intersection for station 136.9. It is also noted that the local total-pressure ratio at the intersection of the flats is nearly the same value at all longitudinal stations and that it also approaches the value of the total-pressure ratio at the surface of the flat. Losses in total pressure associated with probable condensation about the tunnel periphery accompanying large vane openings are again illustrated.

Visual observation of flow conditions along test-section surfaces.-

In conjunction with these total-pressure measurements, flow lines along a flat and along a skirt at the edge of a slot (fig. 2) were obtained by means of oil traces on the respective surfaces. Similarly, flow lines were obtained over the revised diffuser-entrance configuration. The oil traces containing lamp black were, for the most part, located on surfaces in the horizontal plane to eliminate flow lines due to gravity effects. Figure 24 illustrates the general stream lines on the aforementioned surfaces in a three-dimensional cut-away sketch.

In a region immediately upstream of the slot origin (station 107.5) the flow lines on the flat surface are parallel to the center line of the flat. This parallel flow appears to proceed downstream along the central part of the flat until it intersects a flow which converges toward the center of the flat and which appears to originate at the slot origin. The general line of intersection of these flows in the test region indicates an angle of approximately  $30^\circ$  relative to the center line of the flat. Beyond the flow which is converging toward the center of the flat, a flow demarkation line appears close to the edge of the slot. This line, illustrated in the sketch by a continuous dashed line along the entire length of the flat, appears also to originate at the slot

origin and proceeds downstream at approximately a  $1.5^\circ$  angle to the rear of the test region, station 138. The flow at the slot edge beyond this line of demarkation is somewhat toward the slot and does not exceed an angle of  $1.5^\circ$  away from the center line of the flat.

The flow lines along the surface of the skirt which is normal to the surface of the flat and forms the radial boundaries of the slot in the test region (the skirt parallels the center line of the flat at all stations, see figs. 2 and 3) indicate a pattern somewhat similar to that shown along the outer part of the surface of the flat near the edge of the slot. A demarkation flow line appears to originate in the vicinity of the slot origin and progresses downstream toward the diffuser entrance at an angle slightly more than  $2^\circ$  relative to the intersection of the flats. The flow lines on the skirt which are nearer the center of the stream, relative to the aforementioned demarkation line, illustrate a small angular flow toward the center of the stream; whereas the flow lines radially outward of the demarkation line diverge away from the center of the stream at local angles as high as  $30^\circ$  into the surrounding tank.

The described demarkation line or near zero curvature line along the skirt was used directly in locating the radial position of the leading edge of the revised diffuser entrance. Similar flow-line patterns were obtained over the same tunnel surfaces with the original diffuser entrance installed in the tunnel configuration. Figure 25 is a photograph taken of the flow pattern on the slot edge skirt immediately adjacent to the diffuser entrance. It was discerned that the demarkation line, evident in the figure, dictated the position of the mixing region stagnation point on the diffuser entrance. Above this stagnation point severe separation of the flow takes place, whereas below it the flows are actually reversed, traveling upstream and radially outward along the diffuser entrance. At a predesignated tunnel longitudinal station, the measured depth of the demarkation line below the flat surface was used to position the leading edge of the revised diffuser entrance. This location is proved satisfactory by the flow lines illustrated in figure 24 on the skirt in the vicinity of the diffuser entrance, as well as by tuft observations, both of which indicate that the stagnation point of the revised diffuser entrance remains essentially constant on the  $\frac{3}{8}$ -inch leading-edge radius.

### Power Characteristics

Power characteristics of this large-scale facility are shown for variations of diffuser entrance, slot shape, and wall divergence. In addition, a comparison of power per square foot of test-section area for three similar slotted test sections of widely varying scale are presented.

Effect of diffuser entrances.- A comparison of corrected horsepower plotted against Mach number for the original and revised diffuser-entrance configurations is shown in figure 26. All horsepower values are corrected to a stagnation pressure of 2120 pounds per square foot and to a stagnation temperature  $T$  for a particular Mach number based on an average temperature curve from all calibration tests. (See top of fig. 26.) These data were obtained with slot plan form number 1 in the test section and are limited to a horsepower below the 60,000 design maximum by performance limitations of the early tests. The power to produce a given Mach number is appreciably reduced throughout the test Mach number range by use of the revised diffuser entrance configuration. At a Mach number of 0.92 the required horsepower was decreased from 49,900 to 41,700 which is approximately a 16-percent reduction.

Effect of slot-plan-form shape.- The variation in slot shape, although sufficient to alter the uniformity of the flow, was not large enough to enable resultant variations in power to be noted. The originally slotted part of the diffuser was closed from stations 146 to 154 for the revised diffuser entrance configuration and undoubtedly produced a decrease in required power. This change is, however, interrelated with change in diffuser entrance shape and its effects are therefore included in the power data of figure 26.

Effect of wall divergence.- Figure 27 presents a similarly corrected horsepower comparison for wall divergences of  $0^\circ$ ,  $0^\circ 5'$ , and  $0^\circ 10'$  with the tunnel configuration including slot shape number 18 and the revised diffuser entrance. The horsepower required for a Mach number of 0.95 appears somewhat higher with a wall divergence of  $0^\circ 0'$  than that shown for  $0^\circ 5'$  divergence. At this same Mach number the  $0^\circ 10'$  position indicates a required power of the same order as that for the  $0^\circ$  position. Whereas the power curve for the  $0^\circ$  position nearly parallels that of the  $0^\circ 5'$  divergence to the top Mach number shown, the  $0^\circ 10'$  divergence curve crosses that of the  $0^\circ$  position near Mach number 1.0 and then proceeds to approximately parallel the  $0^\circ 5'$  curve to the highest Mach number shown. In the supersonic range the illustrated increase in Mach number is approximately 0.02 per  $5'$  increase in wall divergence at constant power. It is recalled from figure 14, however, that variations in uniformity of flow also increased with increasing wall divergences above about  $0^\circ 5'$ . The  $0^\circ 5'$  wall-divergence position is therefore presently utilized, and Mach numbers up to approximately 1.08 are attained for a corrected horsepower of 62,000.

Power-per-square-foot comparison.- With power data available from three similar transonic test sections of widely divergent sizes, a general comparison of similarly corrected horsepower-per-unit-of-test-section area is presented through the transonic Mach number range in figure 28. The comparison includes data obtained in the 12-inch effective diameter

transonic tunnel (refs. 1 and 2), in the 8-foot transonic tunnel (ref. 3), and in the 16-foot transonic tunnel. The power data for the 12-inch tunnel were computed from the pressure drop between the quiescent chamber upstream of the entrance cone and the downstream end of the diffuser cone. The computation assumed a compression efficiency of 90 percent. The power data from the 8-foot and 16-foot transonic tunnels were obtained from measurements of the electrical input to the tunnel drive systems. The differences in power per unit area here shown include effects peculiar to each tunnel, and are not necessarily a function of scale differences alone. It is believed, however, that a favorable power characteristic associated with increasing tunnel size is generally illustrated.

### CONCLUSIONS

The initial calibration investigation of the Langley 16-foot transonic tunnel indicates the following conclusions:

1. Uniform, transonic, continuously variable flows suitable for testing large-scale models up to a Mach number of 1.08 are established with a specially designed slot plan form and a tunnel-wall divergence angle of  $0^{\circ} 5'$ .
2. The establishment of acceptably uniform supersonic flows with wall-divergence angles greater than approximately  $0^{\circ} 5'$  is not indicated by the results of this investigation.
3. The deviation of the average Mach number in a 6-foot-long model test region from the Mach number indicated by the calibrated static-pressure orifices in the tank does not exceed  $\pm 0.002$ .
4. The flow angularity in pitch at the center line in the test region is negligible for the air-exchange inlet and exit-vane configurations currently in use.
5. The horsepower required for operation of this facility is somewhat less per unit area than for smaller-scale facilities previously reported.
6. The reduction in power required for a given speed which resulted from revision of the diffuser entrance indicates that the diffuser

entrance is a critical region and that further revisions in this region might result in additional power reduction.

Langley Aeronautical Laboratory  
National Advisory Committee for Aeronautics  
Langley Field, Va.

#### REFERENCES

1. Wright, Ray H., and Ward, Vernon G.: NACA Transonic Wind-Tunnel Test Sections. NACA RM L8J06, 1948.
2. Ward, Vernon G., Whitcomb, Charles F., and Pearson, Merwin D.: An NACA Transonic Test Section With Tapered Slots Tested at Mach Numbers to 1.26. NACA RM L50B14, 1950.
3. Wright, Ray H., and Ritchie, Virgil S.: Characteristics of a Transonic Test Section With Various Slot Shapes in the Langley 8-Foot High-Speed Tunnel. NACA RM L51H10, 1951.
4. Ritchie, Virgil S., and Pearson, Albin O.: Calibration of the Slotted Test Section of the Langley 8-Foot Transonic Tunnel and Preliminary Experimental Investigation of Boundary-Reflection Disturbances. NACA RM L51K14, 1952.



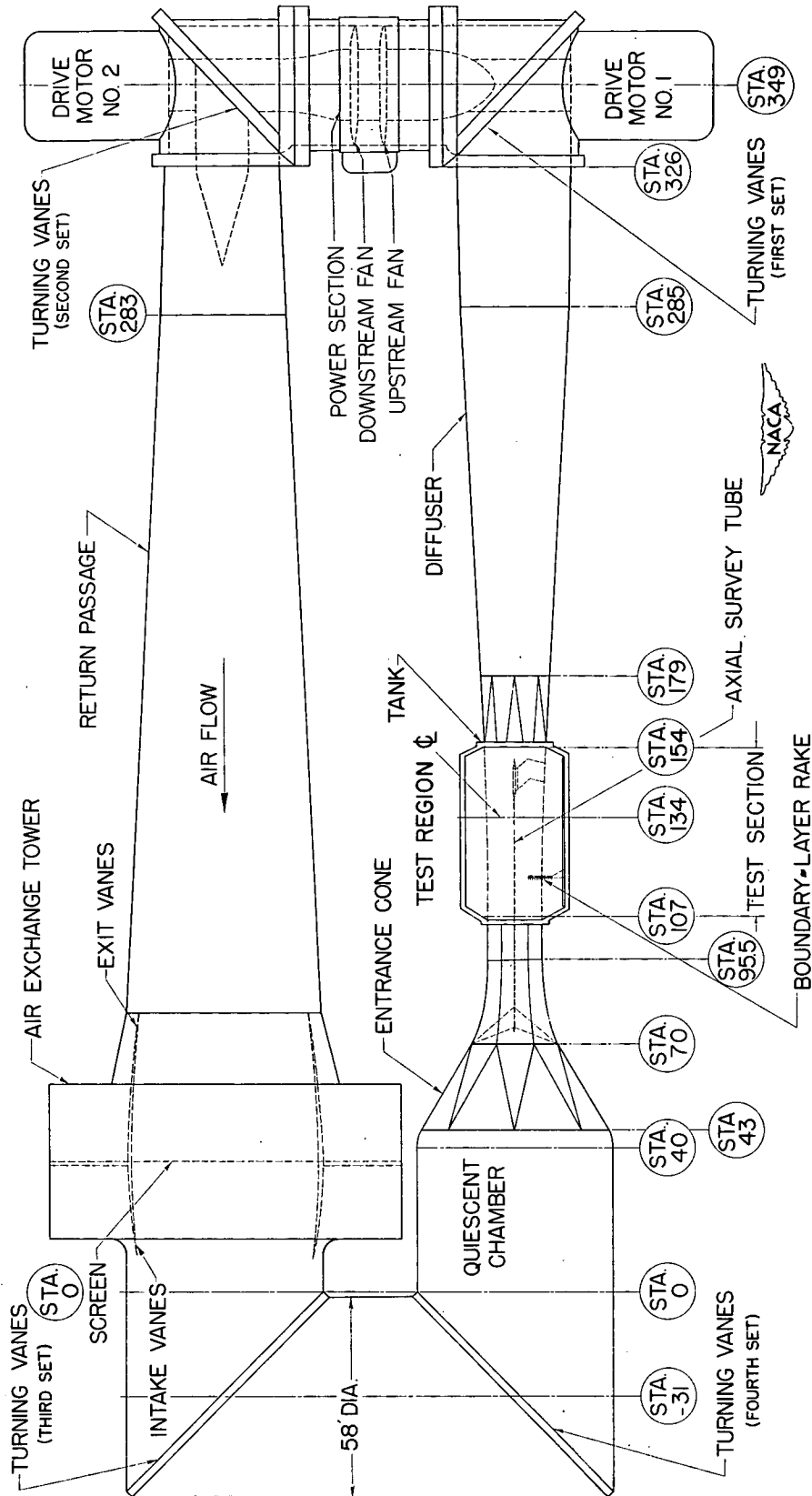


Figure 1.- General schematic view of the Langley 16-foot transonic tunnel, together with pertinent calibration instrumentation.

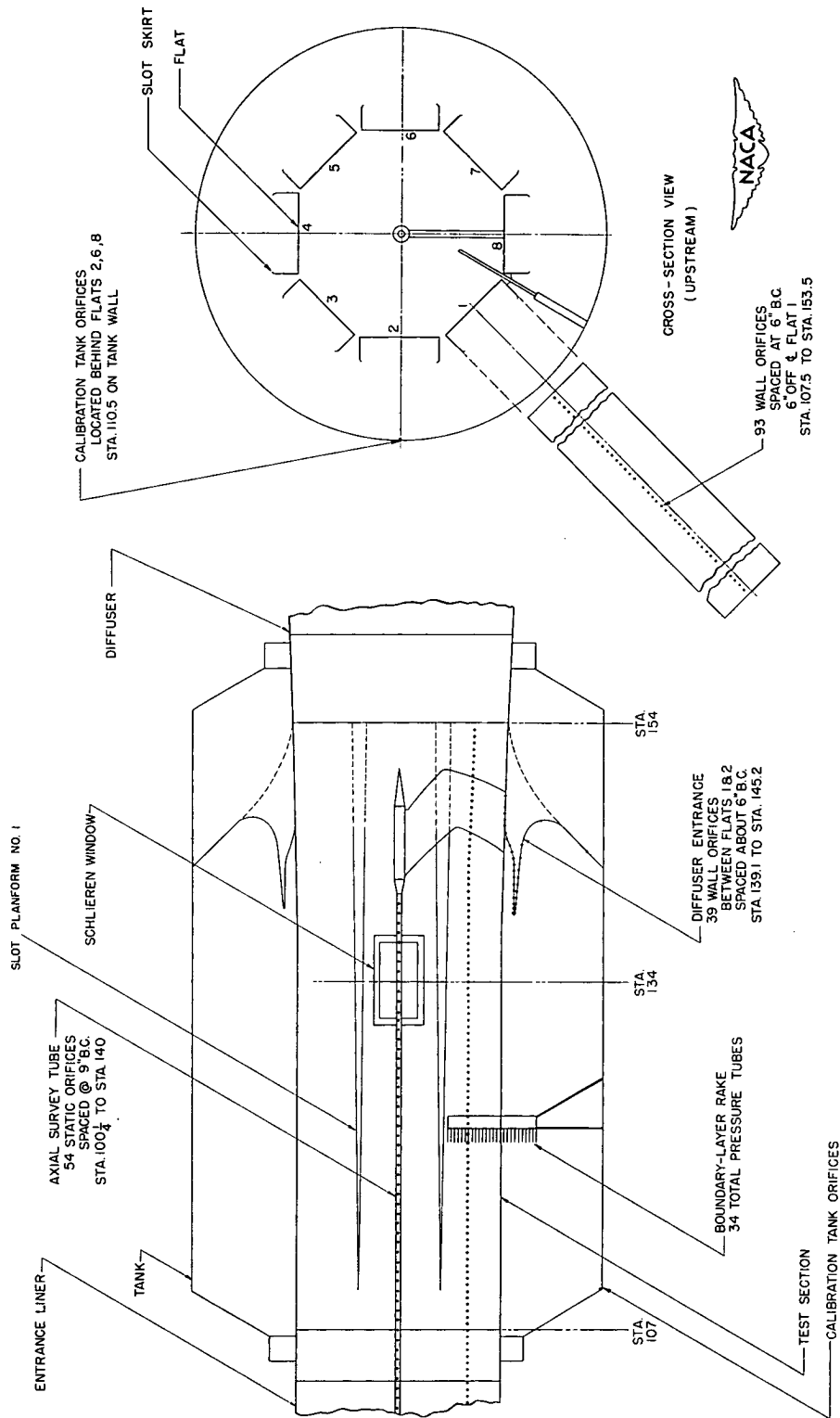


Figure 2.- Schematic sketch of test section of the Langley 16-foot transonic tunnel with calibration instrumentation installed.



Figure 3.- Downstream view of tunnel test section with access hatch in raised position. Slot shape number 18; revised diffuser entrance.

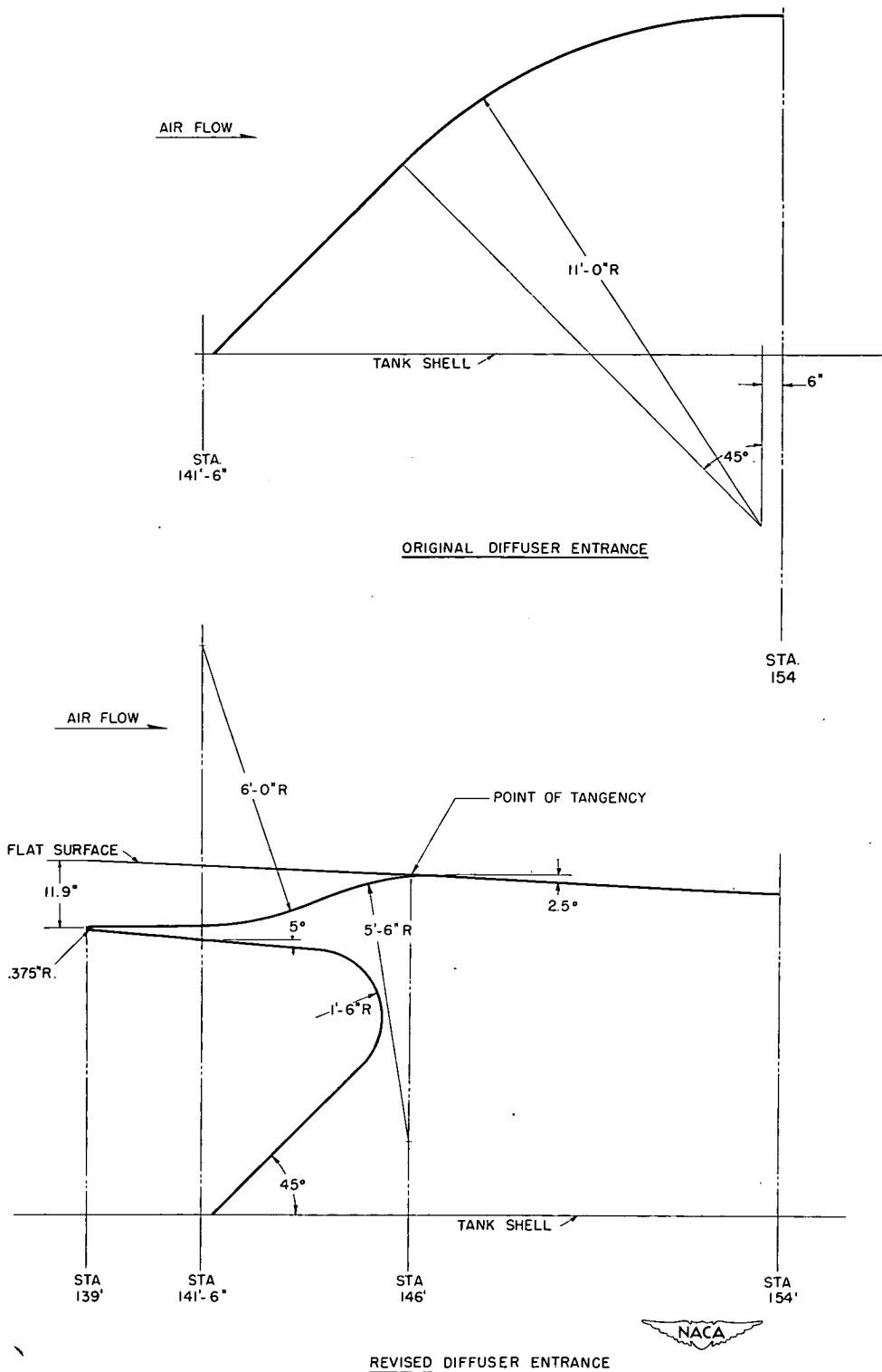


Figure 4.- Schematic sketch of original and revised diffuser entrance shapes taken along radial plane passing through center line of slot.



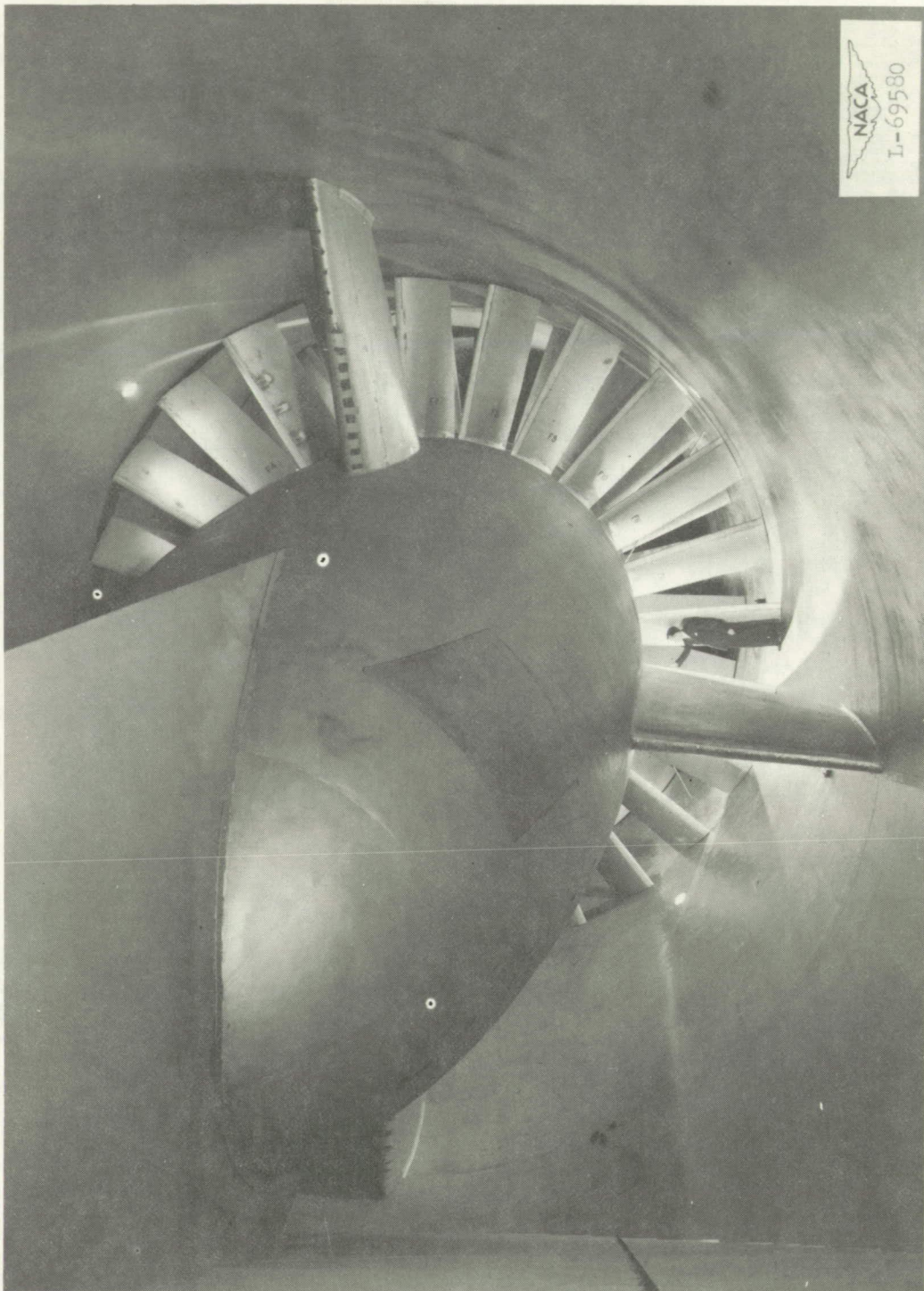
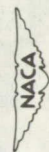
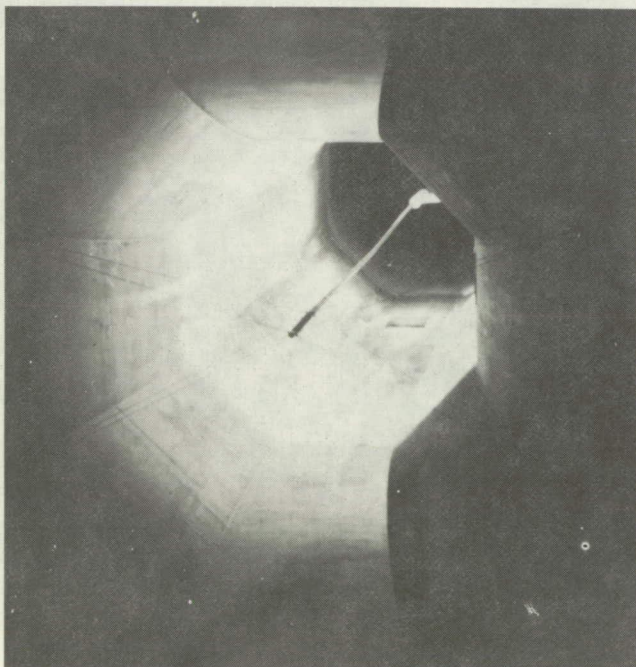
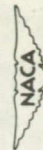
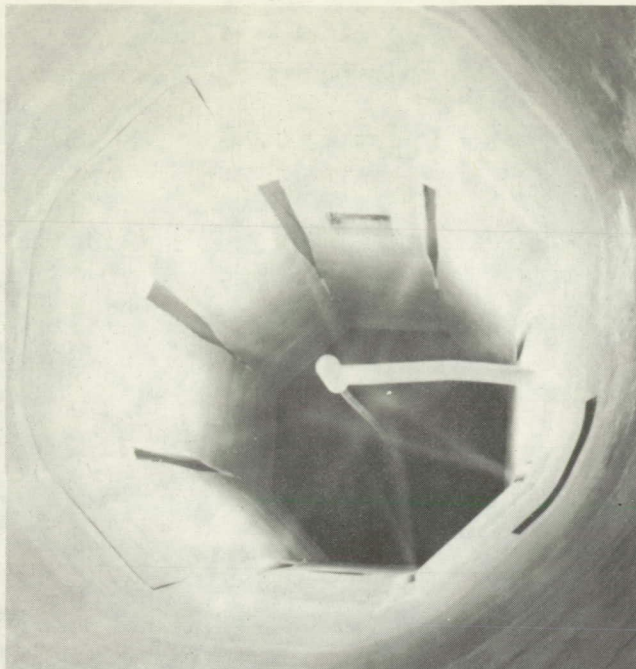


Figure 5.- Downstream view of tunnel power section taken from first set of turning vanes.



L-69575

(a) Downstream view of axial survey tube. Slot shape number 18.

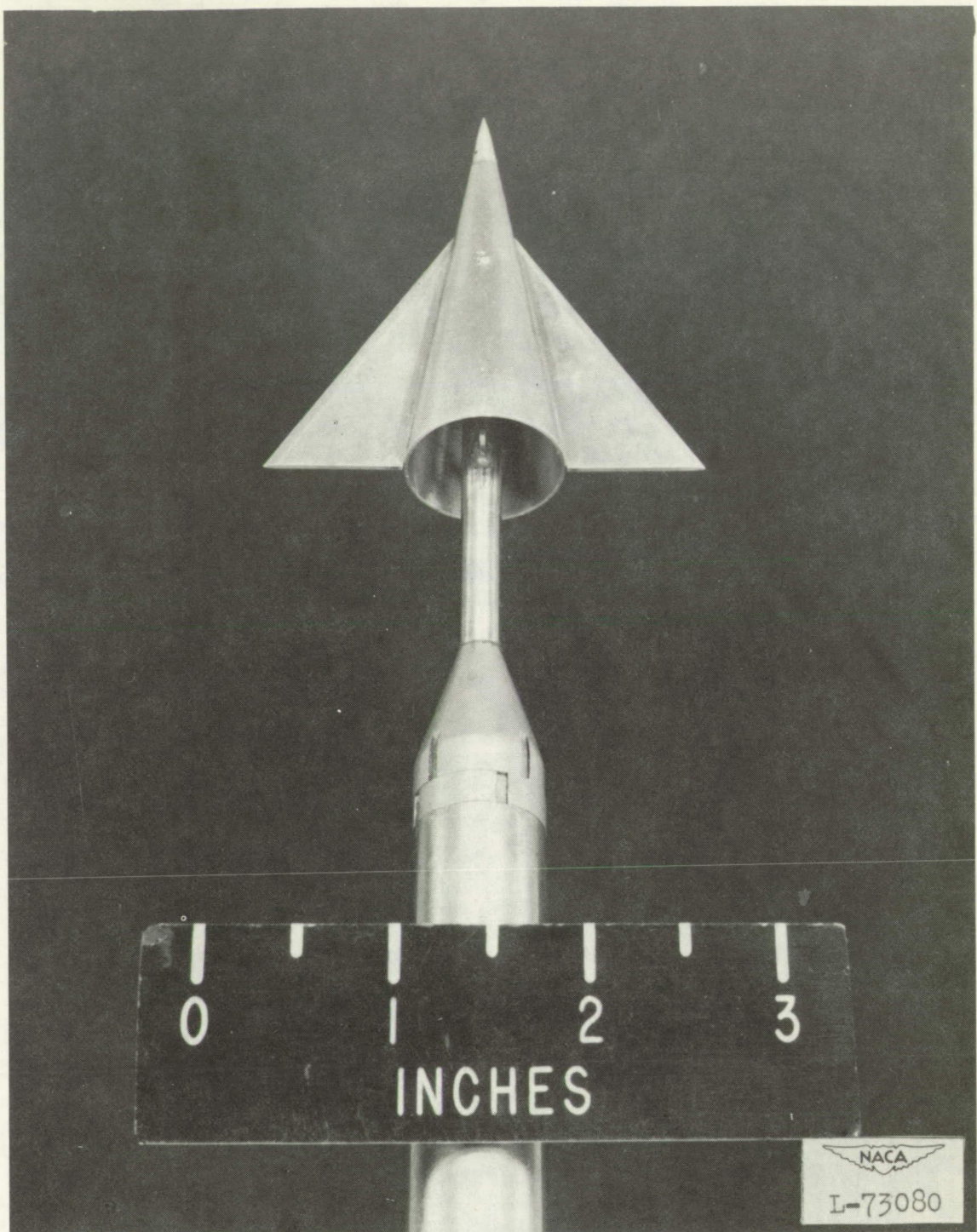


L-69573

(b) Upstream view of axial survey tube. Slot shape number 18.

Figure 6.- Survey instrumentation of the test section of the Langley 16-foot transonic tunnel.





(c) Free-floating angle-of-attack vane.

Figure 6.- Concluded.



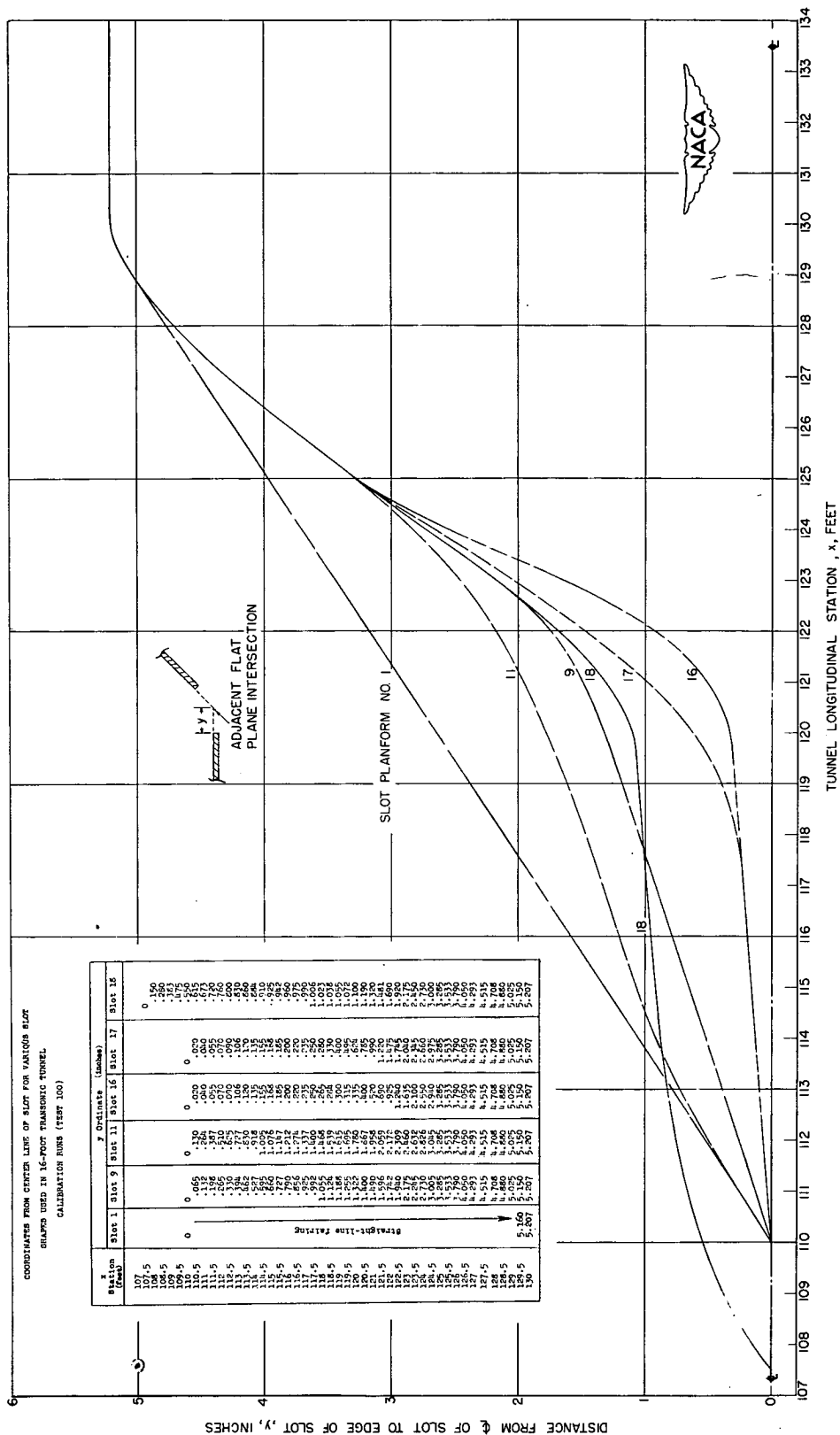


Figure 7.- Table of coordinates and line drawing of slot plan forms tested in the Langley 16-foot transonic tunnel.

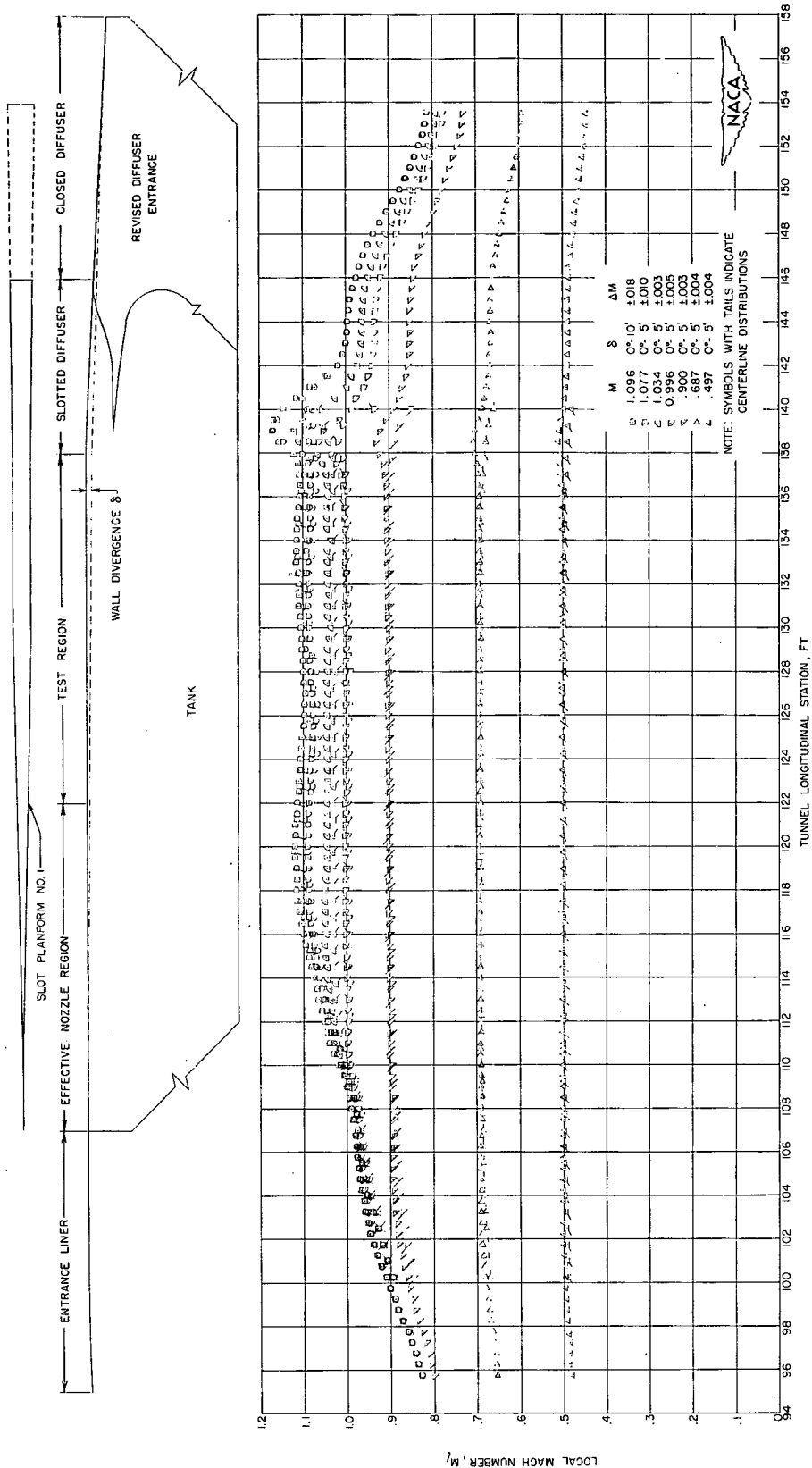


Figure 8.- Longitudinal Mach distributions along wall (6 inches from center line of flat number 1) and along center line of test section of the Langley 16-foot transonic tunnel for slot plan form number 1. Wall divergence is 5 minutes except as noted; axial tube mounted in tunnel with revised diffuser entrance.

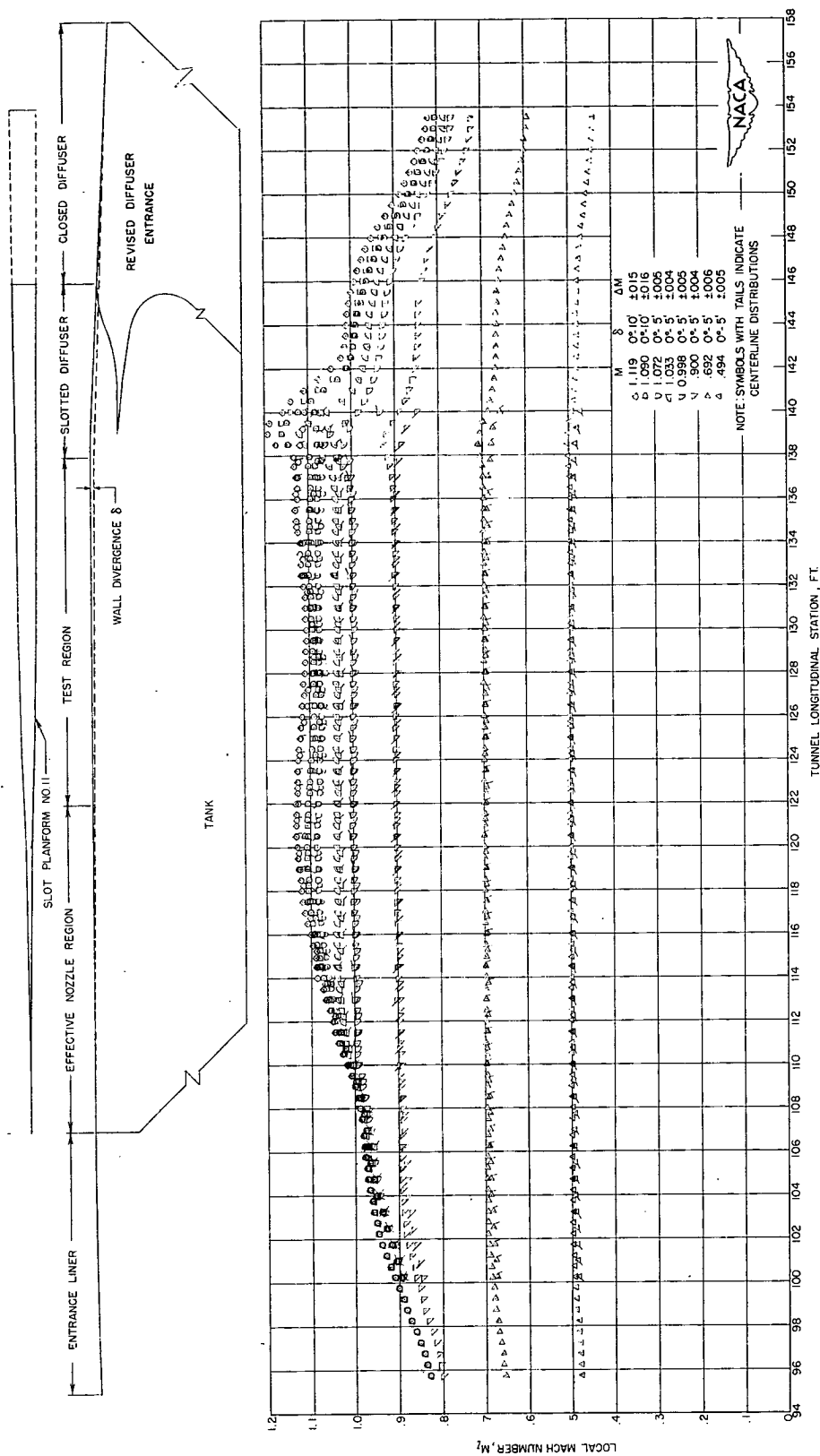


Figure 9.- Longitudinal Mach number distributions along wall (6 inches from center line of flat number 1) and along center line of test section of the Langley 16-foot transonic tunnel for slot plan form number 11. Wall divergence as noted; axial tube mounted in tunnel with revised diffuser entrance.

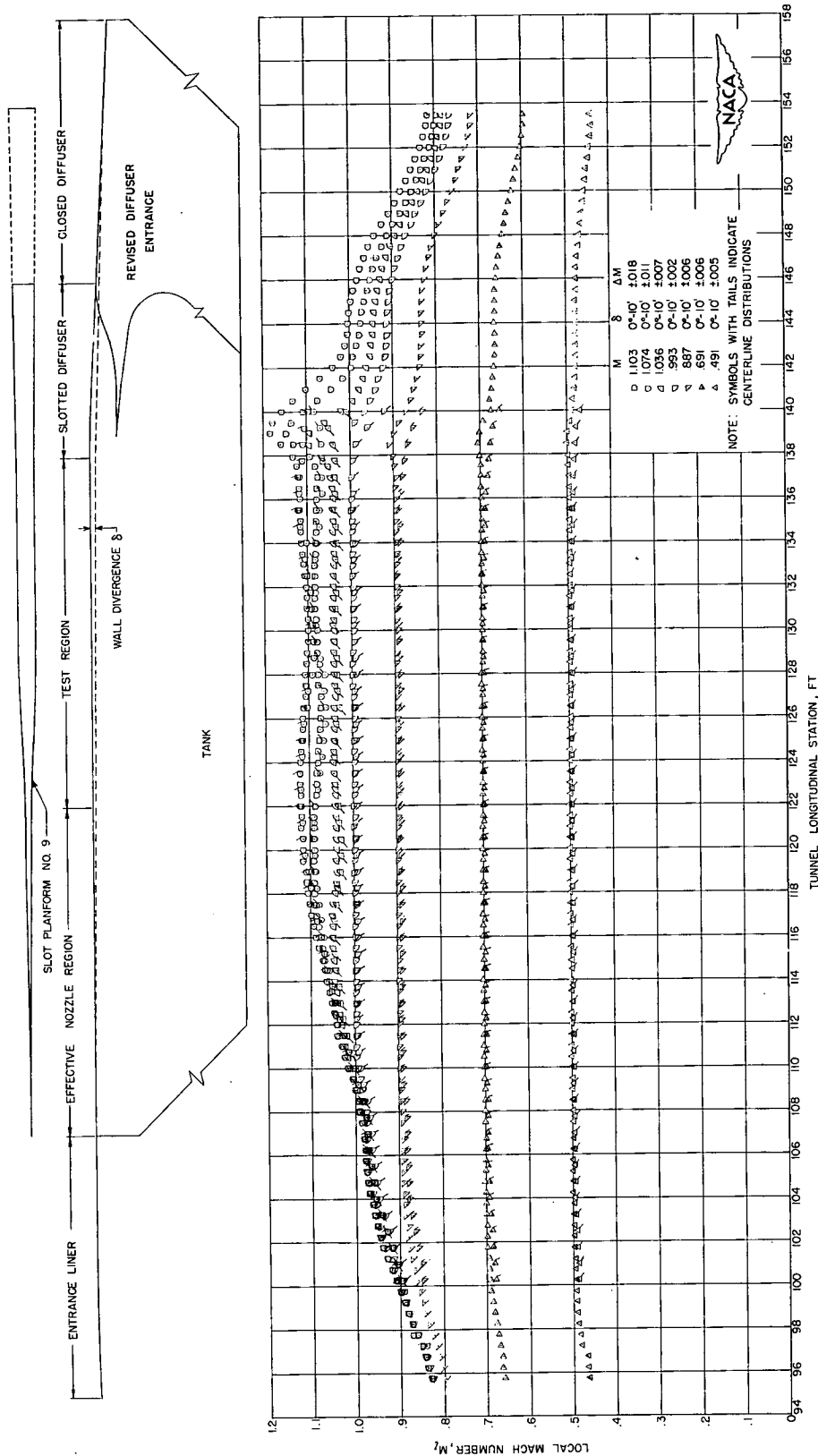


Figure 10.- Longitudinal Mach number distribution along wall (6 inches from center line of flat number 1) and along center line of test section of the Langley 16-foot transonic tunnel for slot plan form number 9. Wall divergence is 10 minutes; axial tube is mounted in tunnel with revised diffuser entrance.

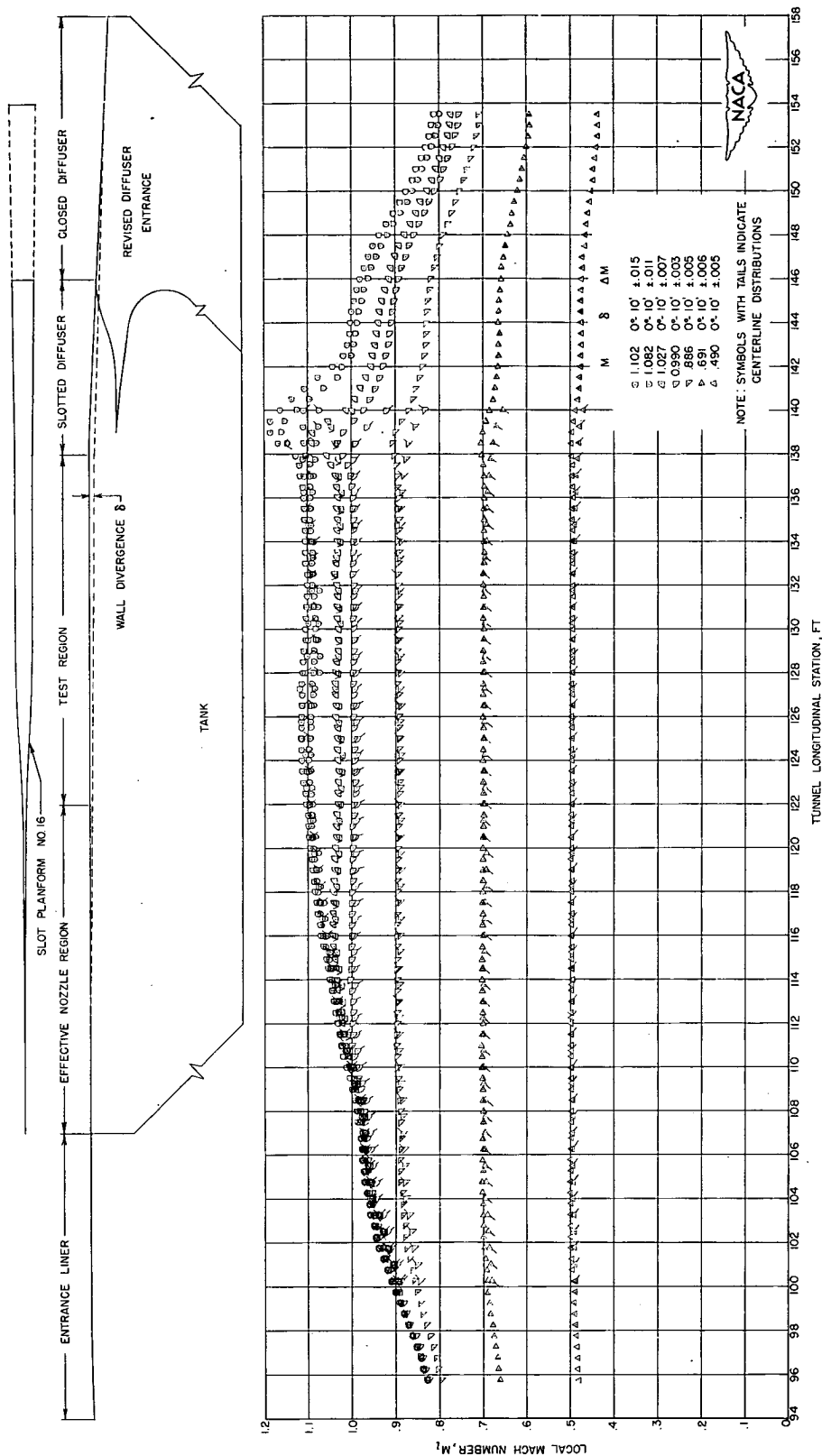


Figure 11.- Longitudinal Mach number distributions along wall (6 inches from center line of flat wall number 1) and along center line of test section of the Langley 16-foot transonic tunnel for slot plan form number 16. Wall divergence is 10 minutes; axial tube mounted in tunnel with revised diffuser entrance.

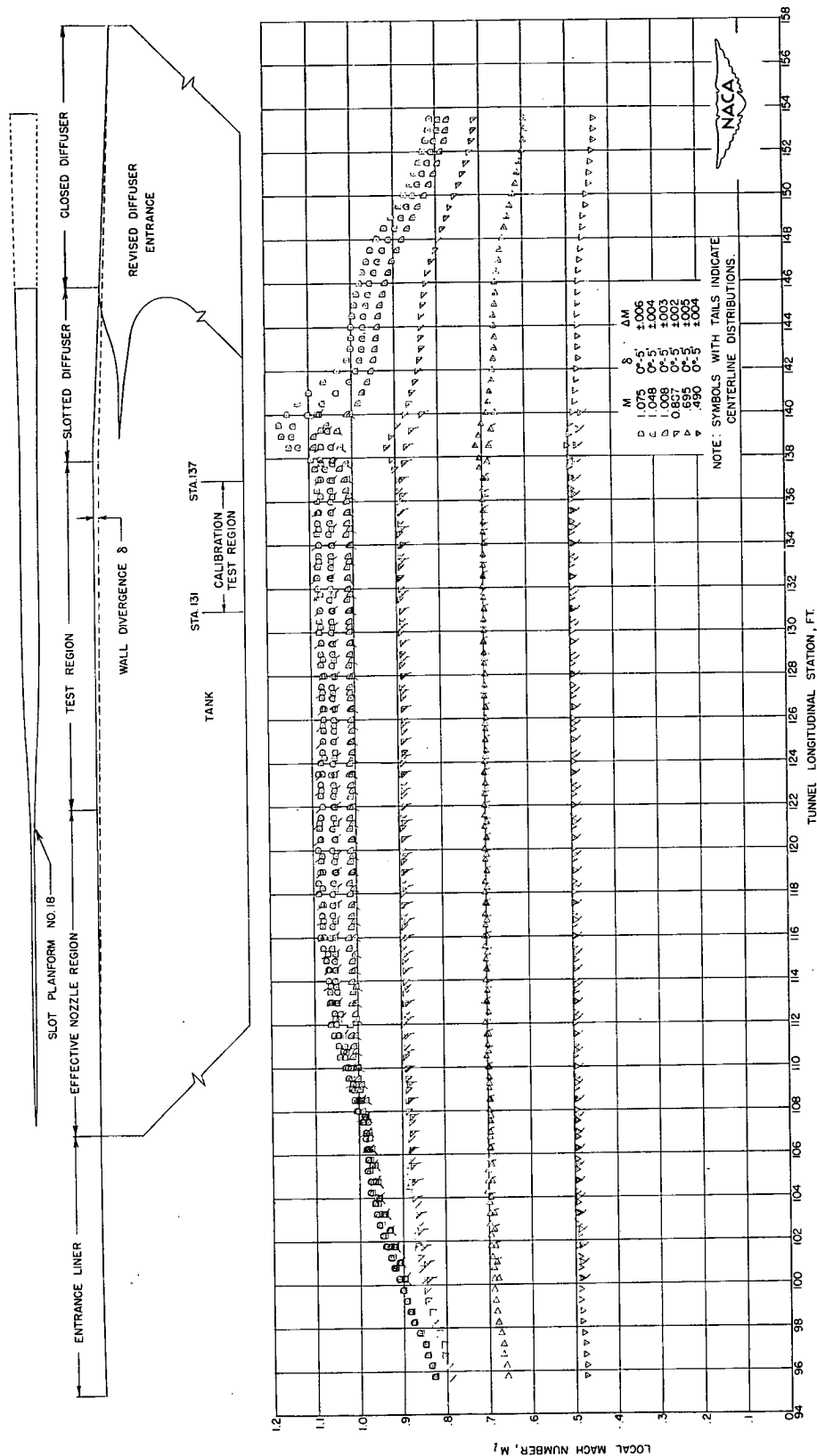


Figure 12.- Longitudinal Mach number distribution along wall (6 inches from center line of flat number 1) and along center line of test section of the Langley 16-foot transonic tunnel for slot plan form number 18. Wall divergence is 5 minutes; axial tube mounted in tunnel with revised diffuser entrance.

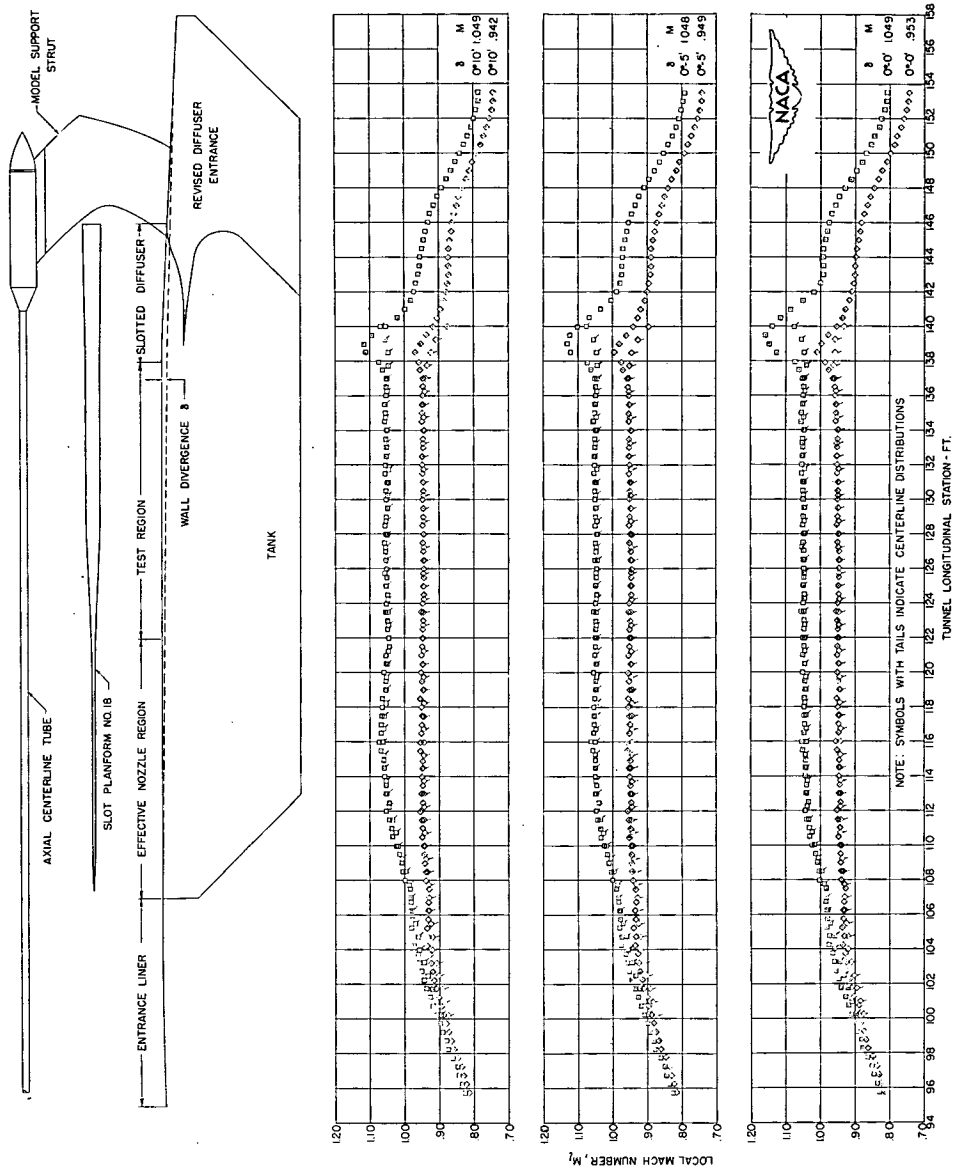


Figure 13.- Longitudinal Mach number distributions along center line and tunnel wall (6 inches from center line of flat number 1) of test section of the Langley 16-foot transonic tunnel with walls at divergence  $\delta = 0^\circ, 0^\circ 5', 0^\circ 10'$ ; subsonic and supersonic Mach numbers.



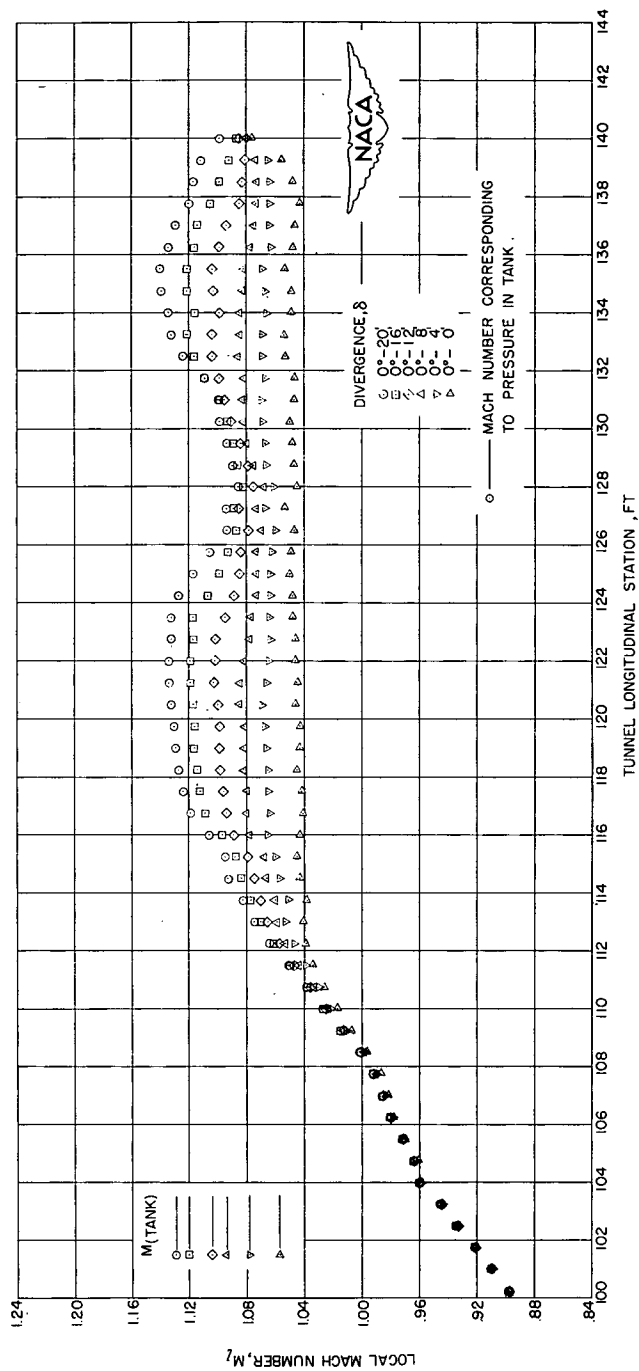
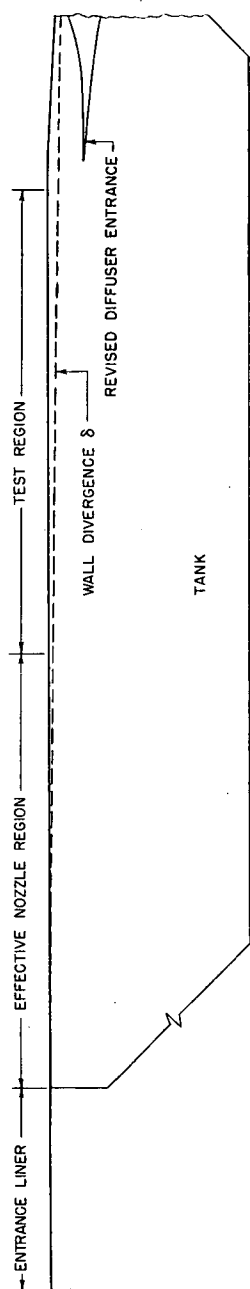


Figure 14.- Comparison of Mach number distributions along center line of the Langley 16-foot transonic tunnel for various wall divergences at top horsepower conditions (hp = 62,000); slot plan form number 18; revised diffuser entrance.

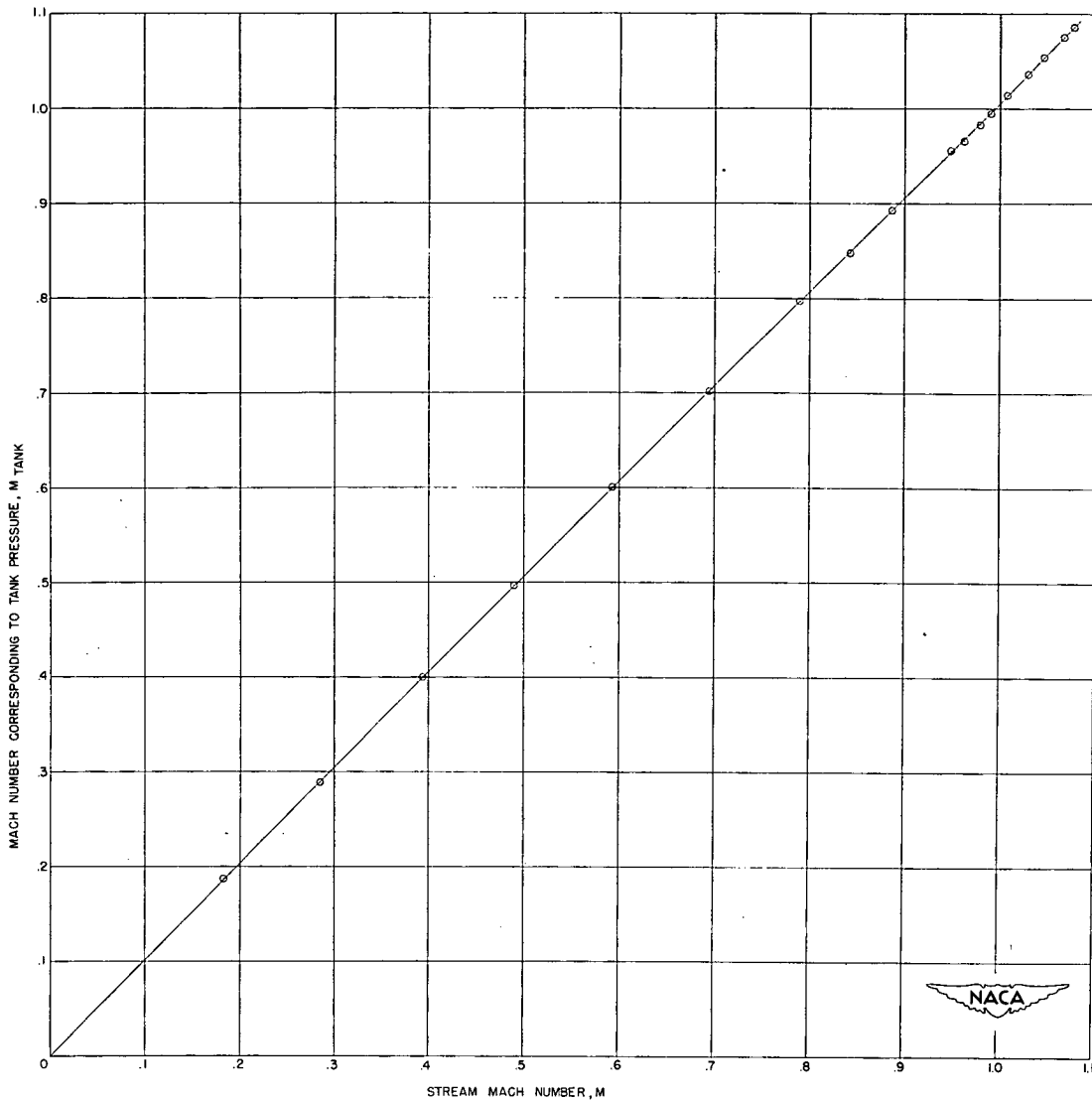


Figure 15.- Calibration of Mach number corresponding to tank pressure  $M_{\text{tank}}$  with the stream Mach number  $M$  which is based on the average pressures as measured on axial tube between stations 131 to 137. Slot shape number 18; wall divergence,  $\delta = 0^\circ 5'$ .

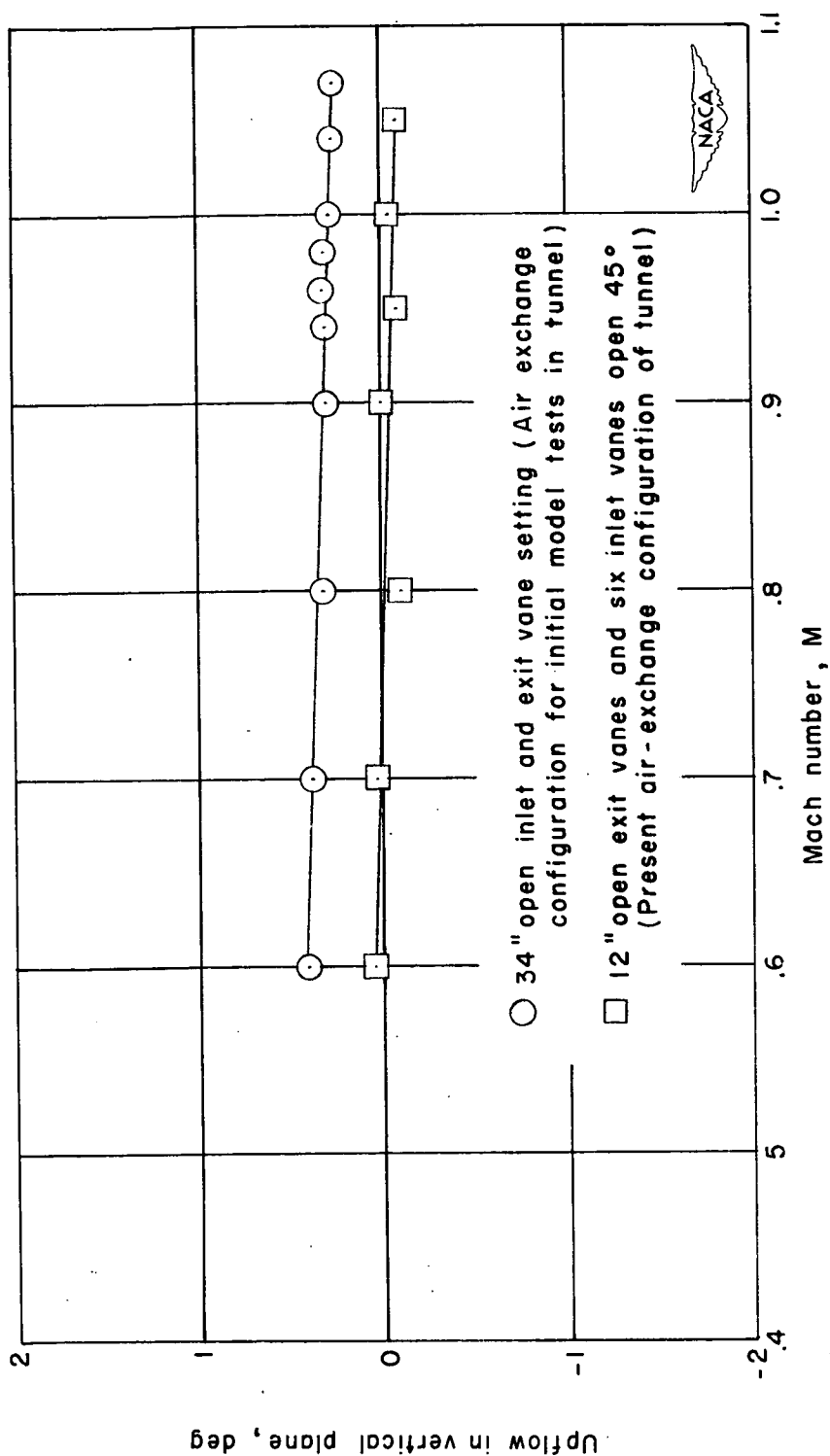


Figure 16.- Flow angularity in the vertical plane in the Langley 16-foot transonic tunnel of various Mach numbers for two different air-exchange inlet and exit vane settings.

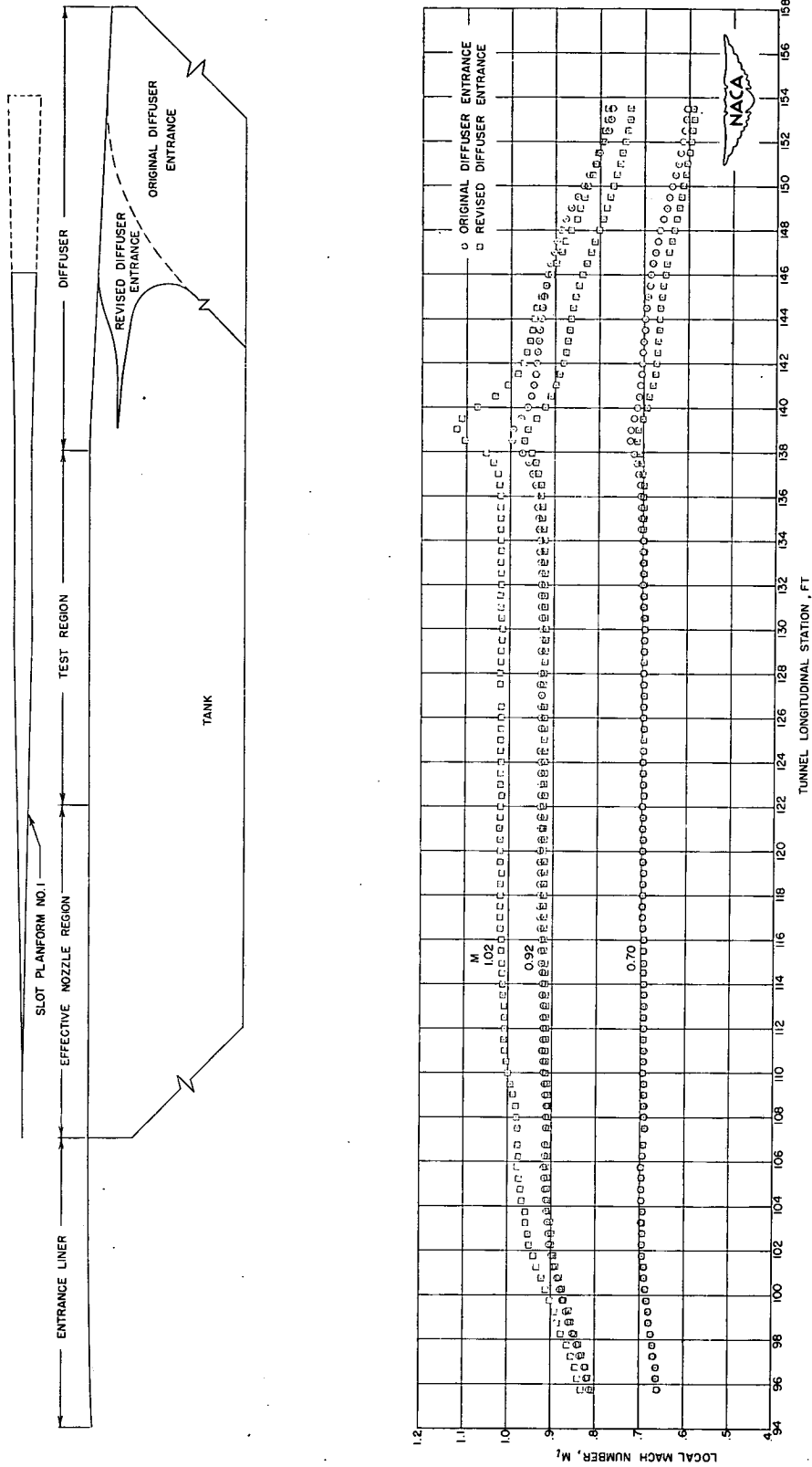


Figure 17.- Comparisons of longitudinal Mach number distributions along wall (6 inches from center line of flat number 1) of the test section of the Langley 16-foot transonic tunnel for the diffuser entrance configurations. Slot plan form number 1; wall divergence,  $\delta = 0^\circ$ .

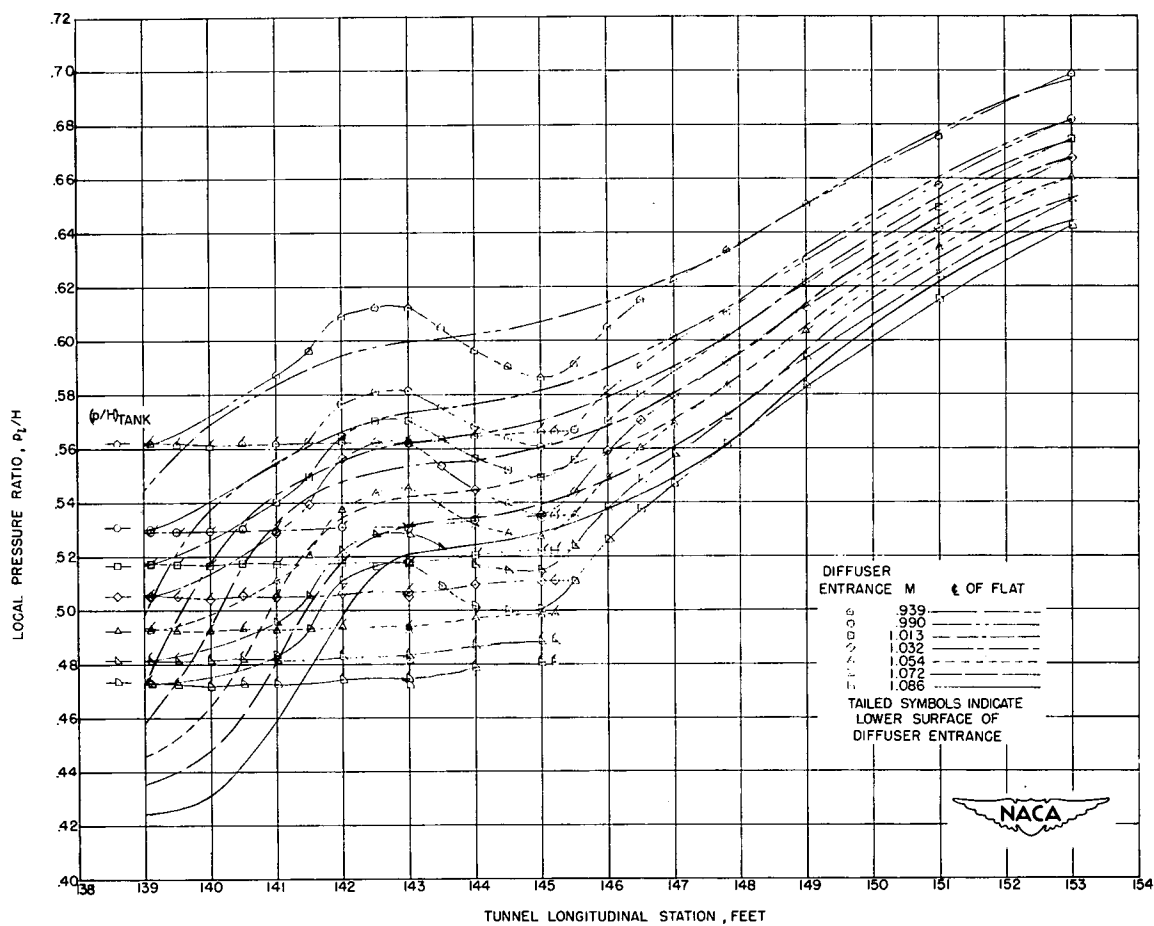
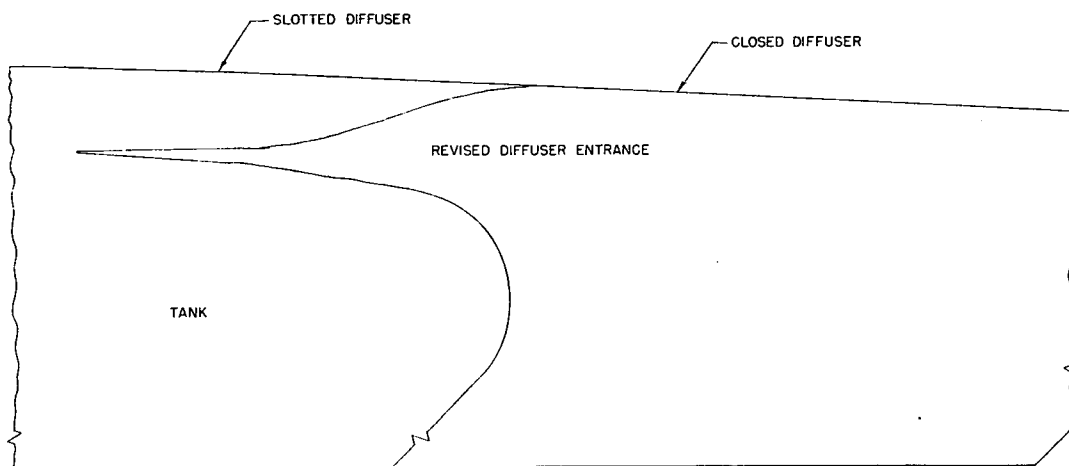


Figure 18.- Comparison of static pressure along center line of upper and lower surfaces of revised diffuser entrance (curve with test points) with corresponding pressures along center line of flat (curve without test points) for several Mach numbers in the Langley 16-foot transonic tunnel. Wall divergence,  $\delta = 0^\circ 5'$ .

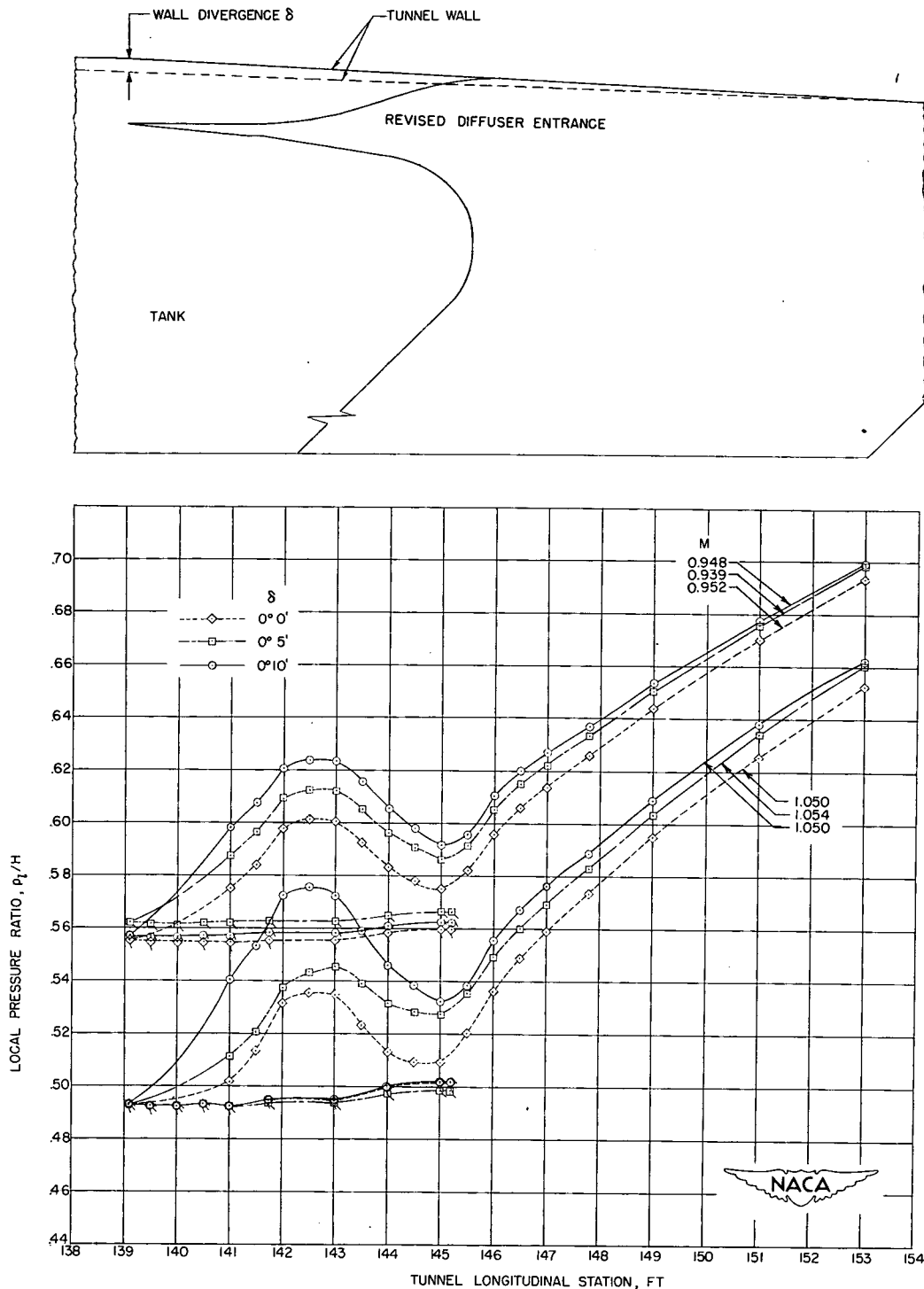


Figure 19.- Comparison of pressure ratio along upper and lower surfaces of revised diffuser entrance for tunnel-wall divergences  $\delta = 0^\circ$ ,  $0^\circ 5'$ ,  $0^\circ 10'$  at similar subsonic and supersonic Mach numbers. Slot plan form number 17.

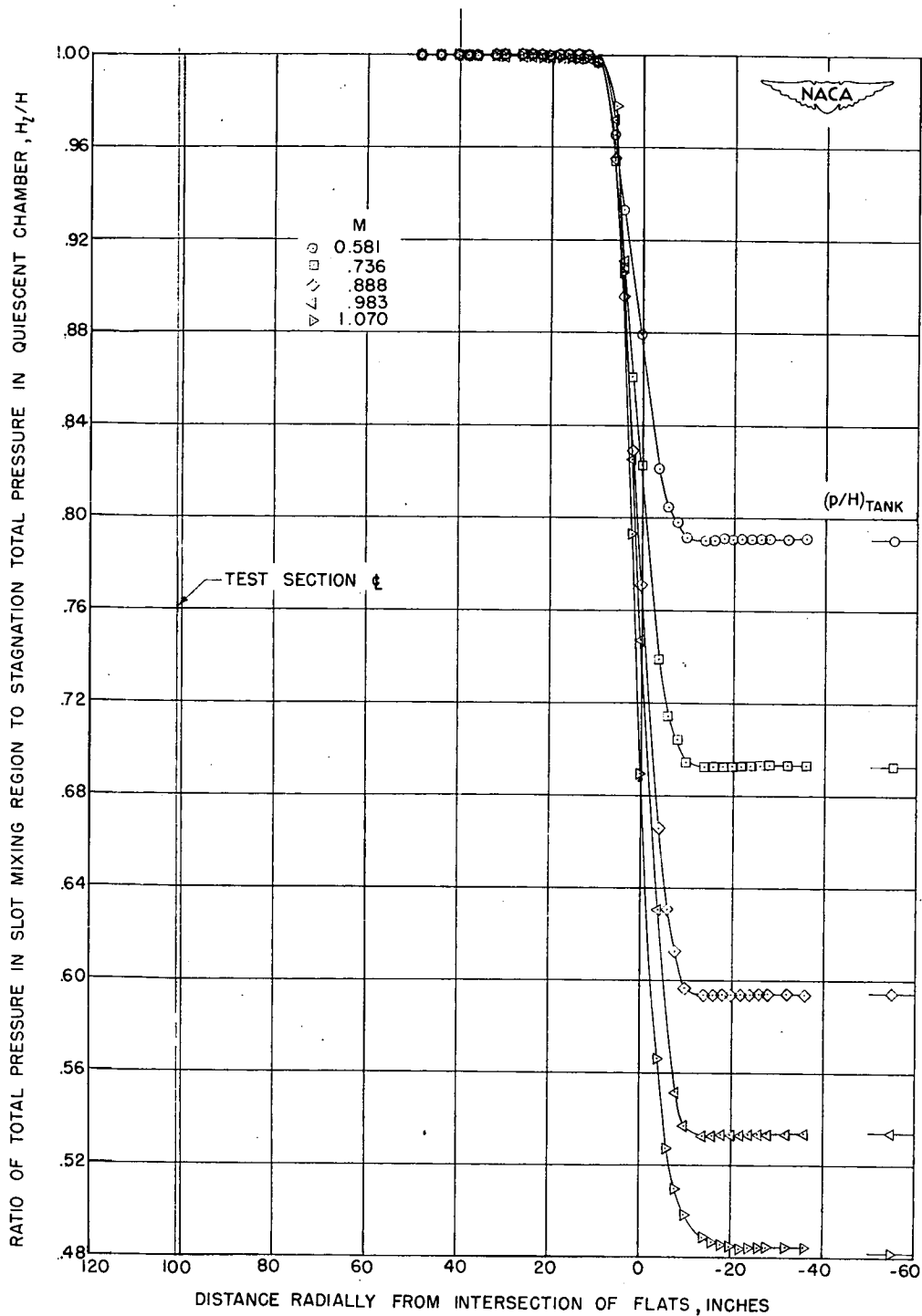


Figure 20.- Total pressure ratios radially through center line of slot at station 126.9 for air-exchange intake and exit vane opening of 12 inches in the Langley 16-foot transonic tunnel for several Mach numbers.

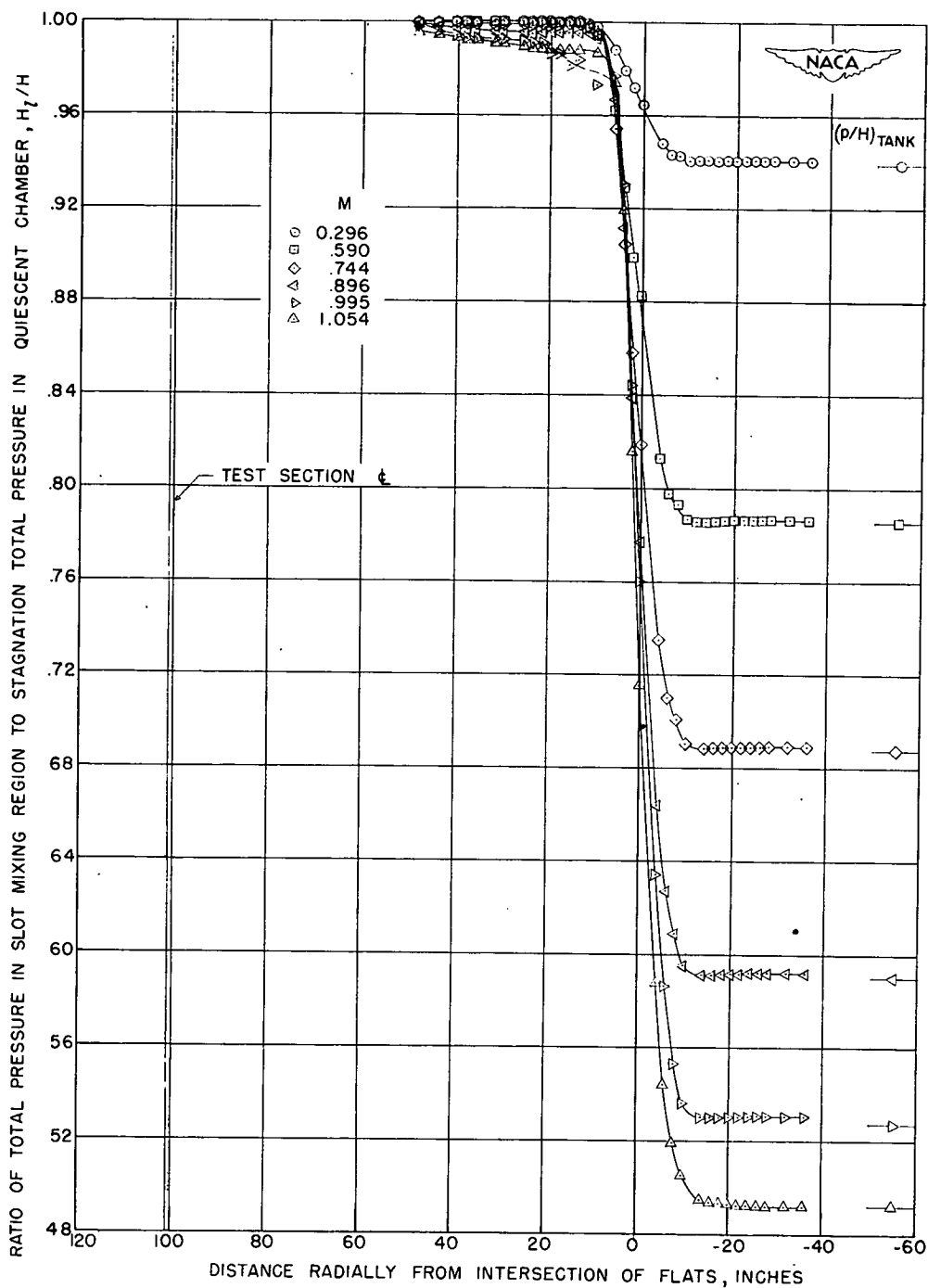


Figure 21.- Total pressure ratios radially through center line of slot at station 126.9 for air-exchange intake and exit vane opening of 36 inches in the Langley 16-foot transonic tunnel for several Mach numbers.



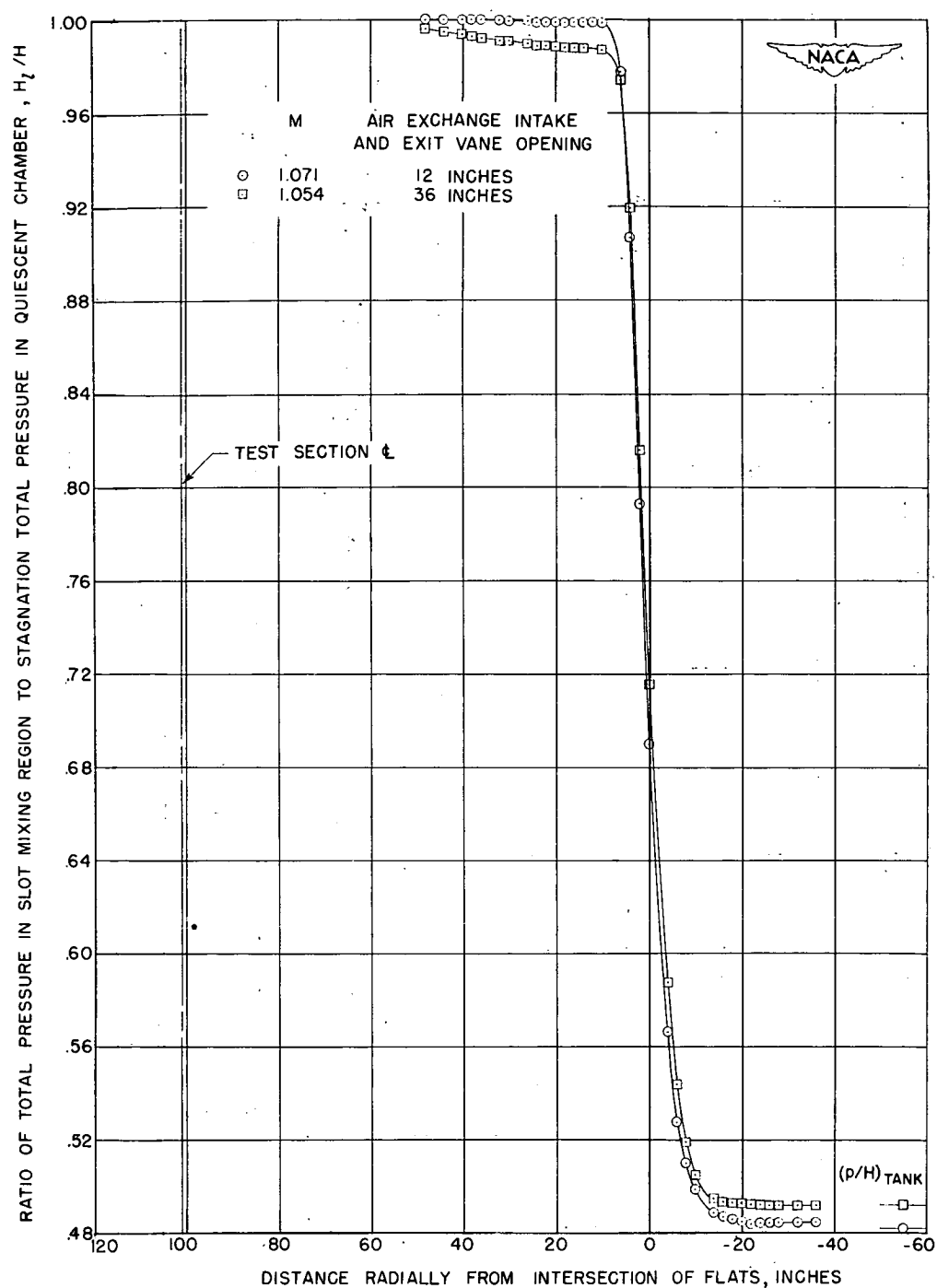


Figure 22.- Comparison of total pressure ratios radially through center line of slot at station 126.9 for air-exchange intake and exit vane openings of 12 inches and 36 inches in the Langley 16-foot transonic tunnel.  $M = 1.071$  and  $1.054$ , respectively.

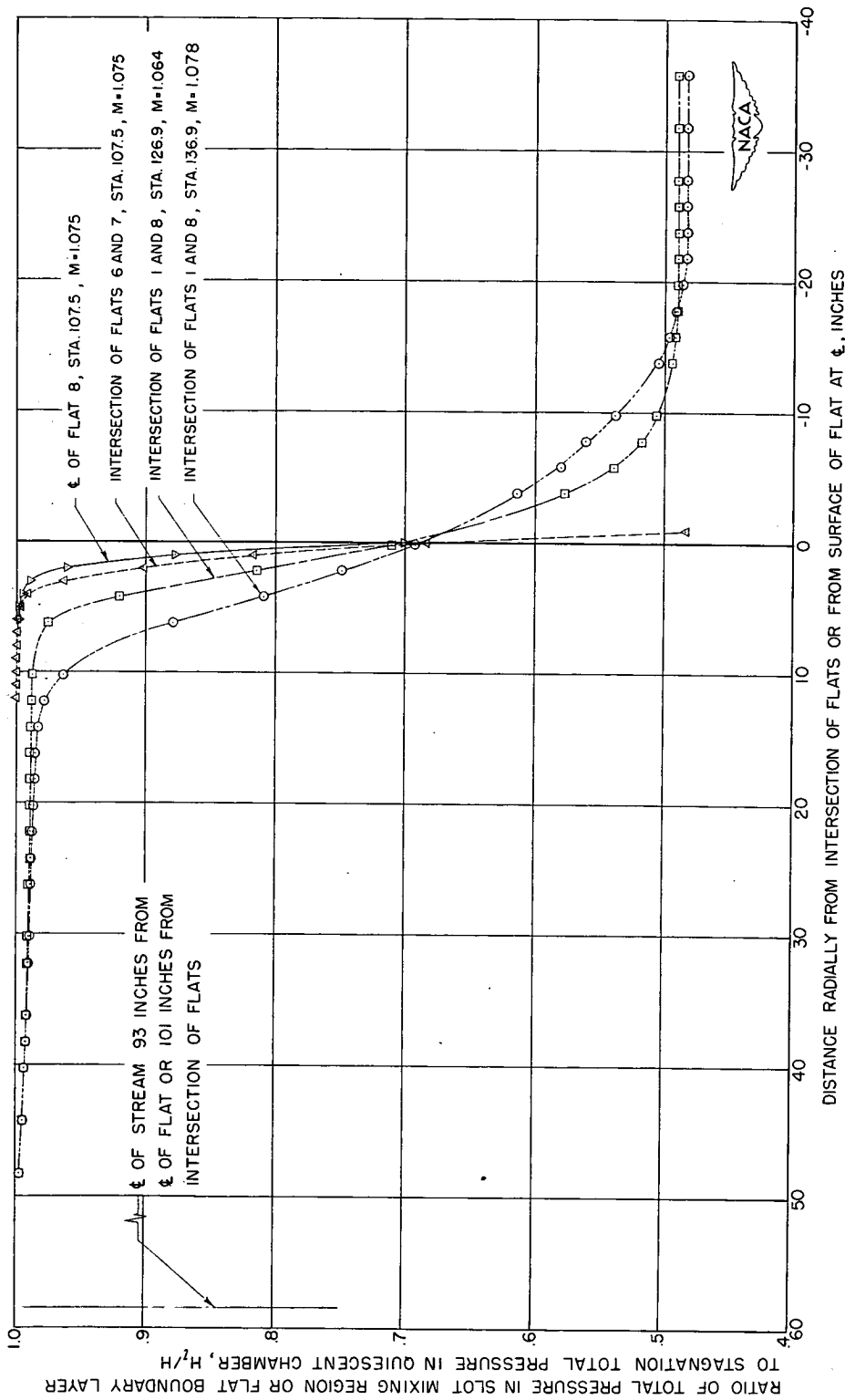


Figure 23.- Comparison of total pressure ratios through center line of slot at stations 107.5, 126.9, and 136.9, together with similar ratios at center line of flat at station 107.5, in the Langley 16-foot transonic tunnel for a supersonic Mach number near 1.07; tunnel empty; air-exchange intake and exit vane opening of 30 inches; slot shape number 18.

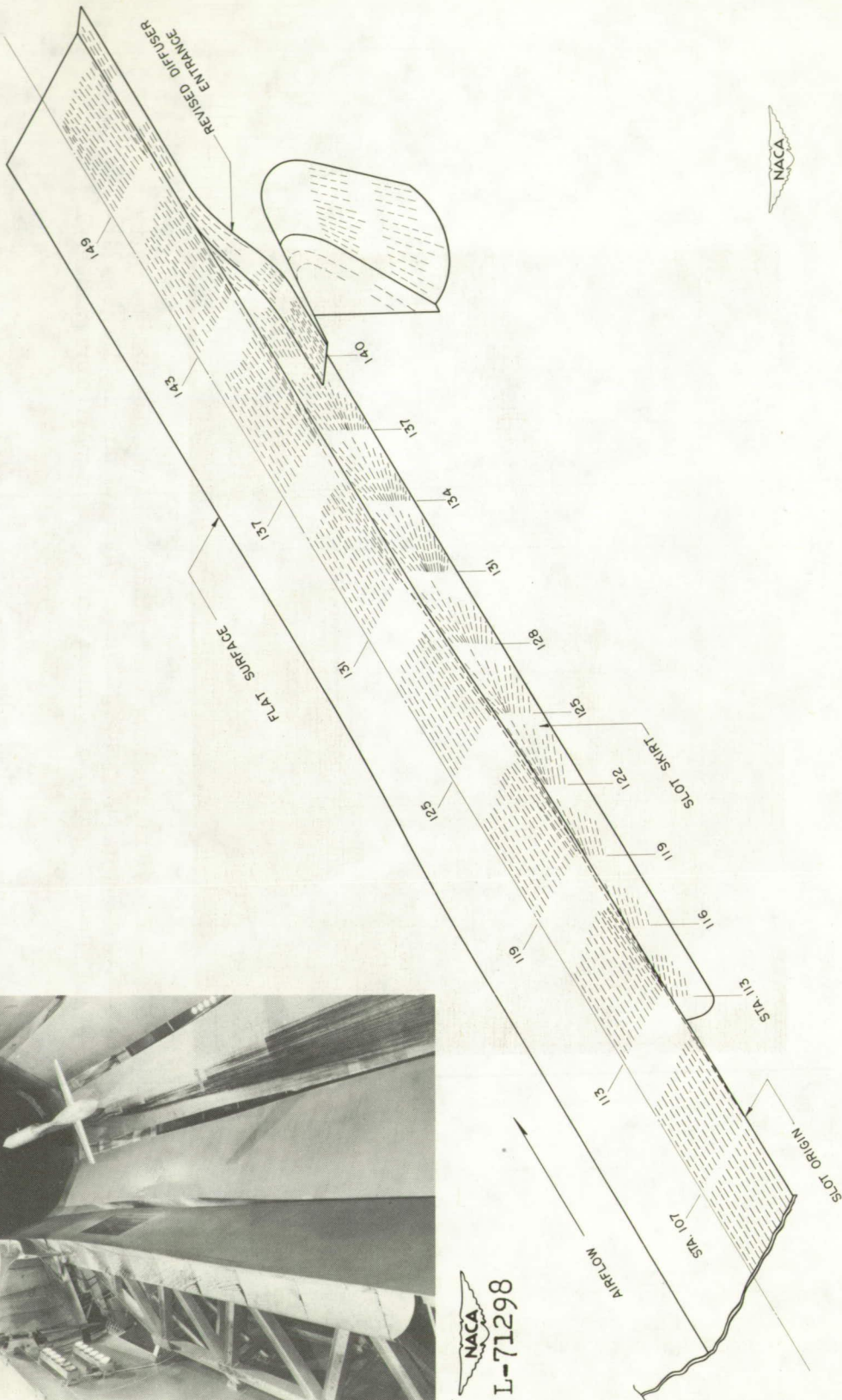
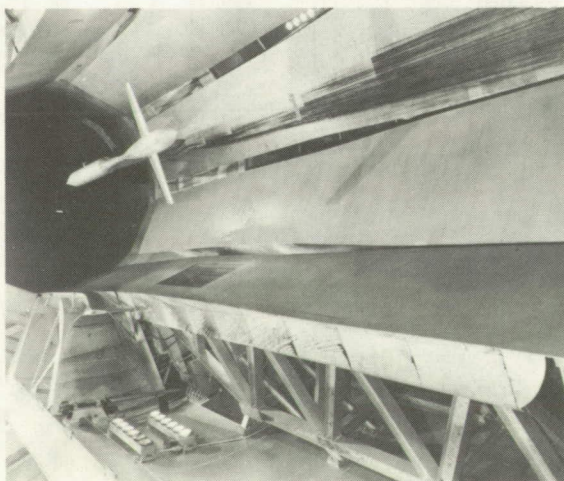


Figure 24.- Flow lines along a flat and along a skirt at the edge of a slot in the Langley 16-foot transonic tunnel. Slot plan form number 18; revised diffuser entrance; wall divergence,  $\delta = 0^\circ 5'$ .

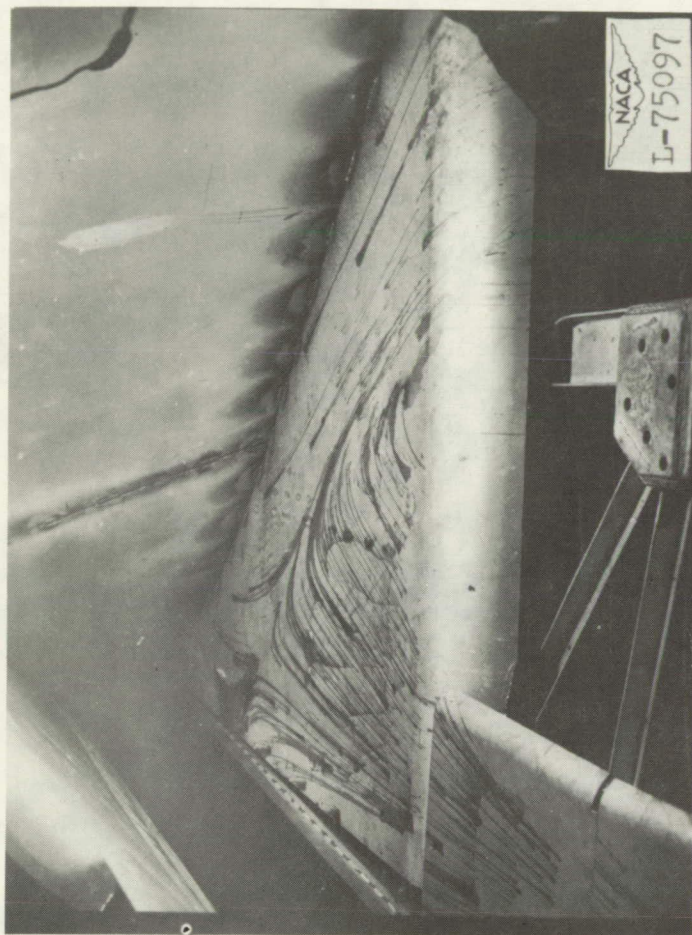


Figure 25.- Flow lines along a horizontal slot edge skirt in the vicinity of the original diffuser entrance in the Langley 16-foot transonic tunnel. Tunnel empty; slot plan form number 1.

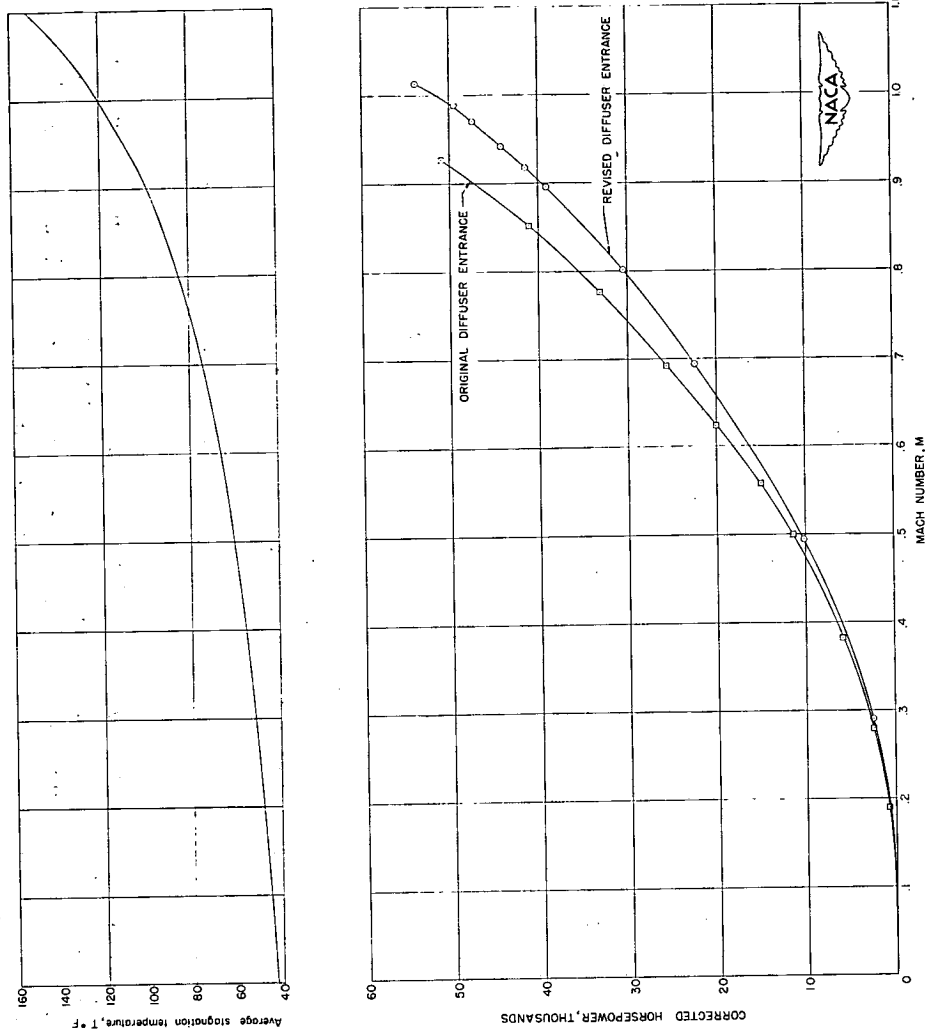


Figure 26.- Comparison of corrected horsepower for original and revised diffuser entrance configurations in the Langley 16-foot transonic tunnel with slot shape number 1;  $H = 2120 \text{ lb/sq ft}$ ;  $T = \text{average stagnation temperature curve for calibration runs; tunnel empty; wall divergence, } \delta = 0^\circ$ .

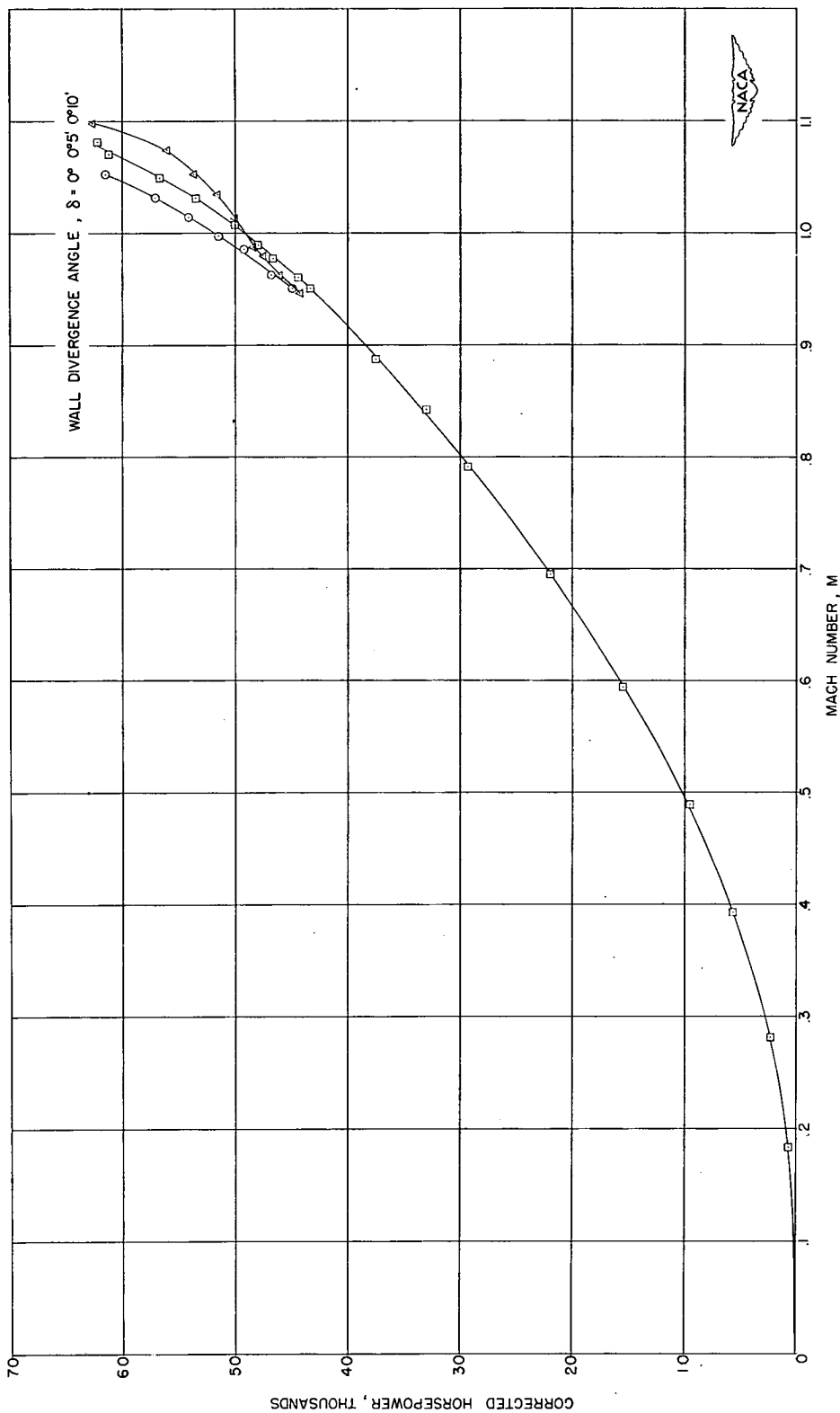


Figure 27.- Comparison of corrected horsepower for wall-divergence angles of  $0^\circ$ ,  $0^\circ 5'$ ,  $0^\circ 10'$  in the Langley 16-foot transonic tunnel with slot shape number 18 and revised diffuser entrance.  $H = 2120$  lb/sq ft;  $T$  = average stagnation curve for calibration runs.

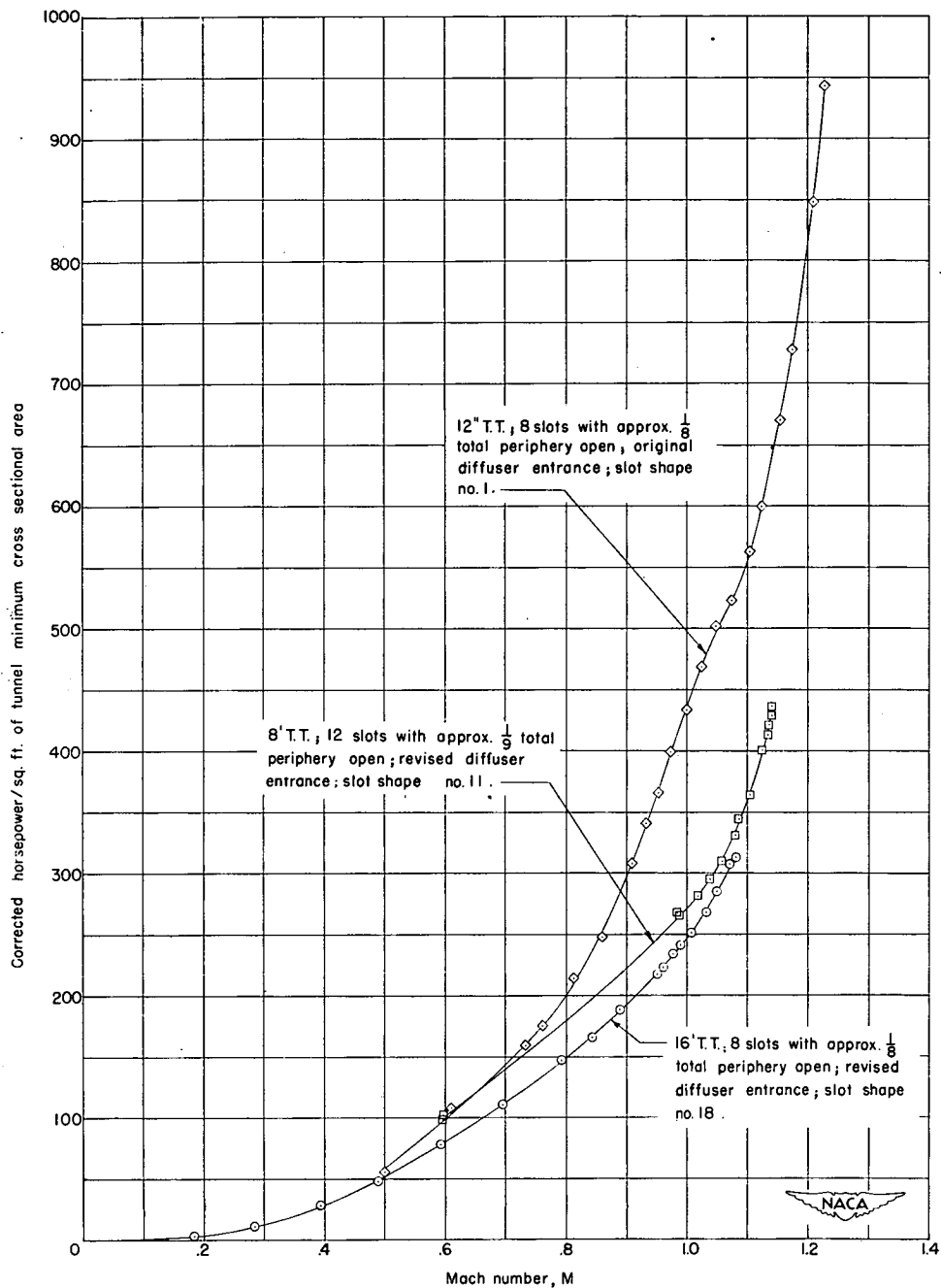


Figure 28.- Comparison of corrected horsepower per square foot of tunnel minimum cross-sectional area for three similar transonic slotted test sections of varying scale.  $H = 2120 \text{ lb/sq ft}$ ;  $T =$  average stagnation temperature curves for calibration runs (see fig. 23); axial tube installed on center line of stream; wall divergence  $\delta$  approximately  $0^\circ 5'$ .